Single-step microfluidic generation of cell-sized giant unilamellar vesicles: Characterization and dielectrophoretic patterning and sorting

Master Thesis

Fredrik Thege

June 30, 2011

LUND UNIVERSITY

Advisor: Dr Johan Nilsson, Department of Electrical Measurements, Lund University
Co-advisor: Dr Abraham P Lee, Department of Biomedical Engineering, University of California, Irvine
Examiner: Dr Thomas Laurell, Department of Electrical Measurements, Lund University

Abstract

Giant Unilamellar Vesicles (GUV) have the potential to play a dominating role in future scientific efforts to understand and model biological systems through the creation of artificial cells. GUV:s span a wide range of possible applications that include their use as biosensors, cell encapsulation agents and biomicroreactors. In order to allow GUV:s to reach their full potential, efficient, reliable and flexible generation methods are essential. Existing bulk methods suffer from many drawbacks while proposed microfluidic methods are still in the developing stages. In this report a novel vesicle generation technique is proposed, based on previously published principles.[28][31][29] Vesicles are created from double emulsion templates generated in a single-step flow focusing microfluidic device. The double emulsion generation was characterized and shown to allow generation in both the dripping and jetting regime of droplet generation. The lipid bilayers were created by extraction of excess solvent. The method allowed creation of vesicles in a wide size range (6.5-45μm) at high generation frequencies (300-3500Hz). The created vesicles were characterized using fluorescent methods and quantification of the permeability of the created membranes. Dielectrophoresis (DEP) was proposed and explored as a general method to manipulate generated vesicles. DEP allows for non-invasive, reversible and complex manipulation of vesicles. Patterning and size selective binary sorting using DEP was shown.

Contents

I Introduction and Background **5**

1 Purpose **5**

2 Vesicles **5**
2.1 Definitions and general considerations . . . 5
2.2 Applications of GUVs . . . 8
2.2.1 Artificial cells . . . 8
2.3 Membrane properties and components . . . 9
2.3.1 Phospholipids . . . 9
2.3.2 Proteins . . . 10
2.3.3 Membrane permeability . . . 10

3 Vesicle generation **11**
3.1 Existing methods . . . 12
3.1.1 Gentle hydration and electroswelling . . . 12
3.1.2 Water-in-oil emulsion transfer method . . . 13
3.1.3 Methods involving microfabrication . . . 13

4 Microfluidic generation of vesicles **14**
4.1 Microfluidics . . . 15
4.2 Laminar flow . . . 15
4.3 Droplet microfluidics . . . 15
4.3.1 Droplet generation . . . 15
4.3.2 Double emulsion generation . . . 18
4.4 Vesicle generation through solvent extraction . . . 18
4.5 Pumping . . . 18

5 Dielectrophoresis, DEP **19**
5.1 DEP of vesicles . . . 19
5.2 Theory . . . 20
5.3 DEP trapping . . . 21

II Materials and Methods **23**

6 Device fabrication **23**
6.1 Silicon wafers . . . 23
6.2 Photoresists . . . 23

6.3 Masks . . . 23
6.4 Soft lithography . . . 24
6.5 PDMS molding . . . 24
6.6 Device assembly . . . 24
6.7 Surface treatment . . . 25
6.8 Gold electrodes . . . 26

7 Device designs **26**
7.1 Junction type N . . . 26
7.2 Junction type A . . . 26
7.3 Junction type B . . . 27

8 Oil phase components **27**
8.1 Phospholipids . . . 29
8.2 Membrane dye . . . 29

9 Aqueous phases **30**
9.1 External phase . . . 30
9.2 Internal phase . . . 30

10 Experimental setup **31**
10.1 Vesicle generation . . . 31
10.1.1 Solvent extraction . . . 31
10.2 Osmotic pressure shock . . . 32
10.3 DEP patterning . . . 33
10.4 Size selective DEP trapping . . . 34

III Results and Discussion **35**

11 Vesicle generation **35**
11.1 Device design . . . 35
11.2 Vesicle size . . . 35
11.3 Generation frequency . . . 38
11.4 Device comparison . . . 40

12 Vesicle characterization **41**
12.1 Osmotic pressure shock . . . 42

13 DEP **44**
13.1 Particle modeling . . . 44
13.2 DEP patterning . . . 45

13.3 Selective DEP trapping 48

IV Conclusion **50**

Part I
Introduction and Background

1 Purpose

The purpose of this Master Thesis is to develop a microfluidic device capable of generating cell sized GUVs at high generation frequencies. Furthermore, DEP will be explored as a possible way to allow patterning and selective trapping of the GUVs generated.

2 Vesicles

2.1 Definitions and general considerations

The term vesicle comes from the latin word *vesicula*, meaning small bladder. Vesicles are supramolecular assemblies consisting of a small aqueous compartment enclosed in a molecular envelope. The molecular envelope is made up from one or more bilayers of amphiphilic molecules, creating membranes surrounding the compartment. Vesicles with only one bilayer are referred to as being unilamellar while vesicles with multiple bilayers are referred to as oligolamellar or multilamellar vesicles. In this report only unilamellar vesicles will be considered.

Most commonly the amphiphilic molecules that constitute the membrane layer are phospholipids, such as those present in biological membranes. Diacyl phospholipids have two fatty acid chains, comprising the hydrophobic part of the molecule, a phosphate group and a charged or non-charged head group, comprising the hydrophilic part of the molecule. The amphiphilic nature of the phospholipids results in a spontaneous self organization into laminar bilayer structures. This subgroup of vesicles is commonly referred to as liposomes or lipid vesicles, see figure 1.

Other types of vesicles exist, such as polymersomes (amphiphilic coblock polymers make up the membrane) and surfactant vesicles (synthetic surfactants make up the membrane), but in this report the term vesicles will refer exclusively to liposomes. [33]

Vesicle sizes Unilamellar vesicles come in a wide range of sizes. Small Unilamellar Vesicles (SUVs) is the category of the smallest vesicles. The lower size limit of SUVs correspond to the case where interior volume of the vesicle is entirely filled up by the head groups of the phospholipids making up the membrane. SUVs are typically on the order of 25nm in size. The extreme degree of curvature in SUVs generally make them less stable than larger vesicles. The degree of curvature also result in the internal monolayer containing considerably fewer amphiphilic molecules than the external.

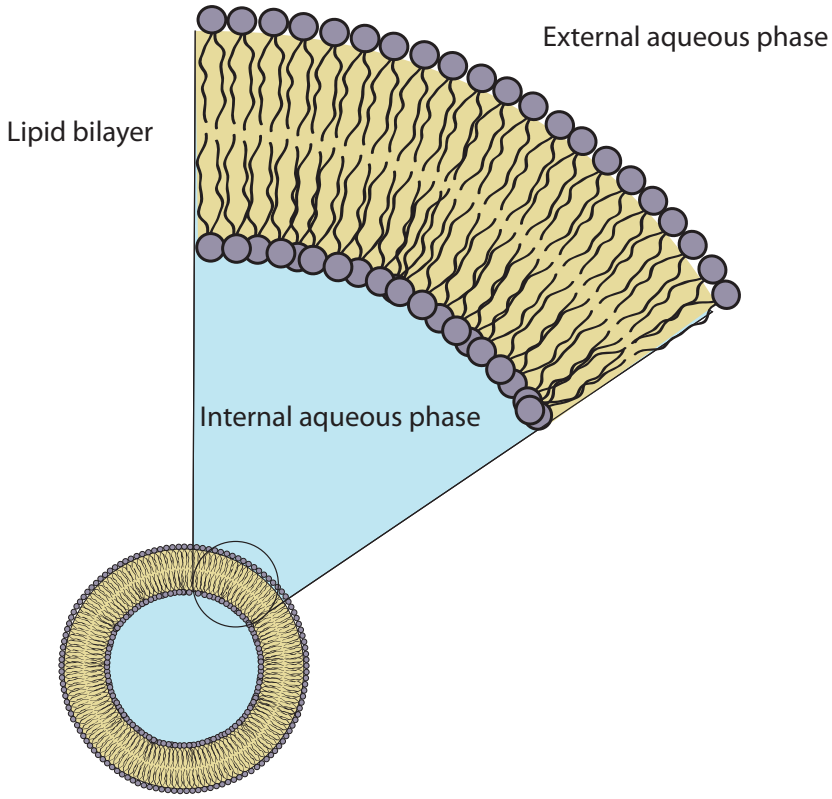

Figure 1: Schematic illustration of an unilamellar lipid vesicle. The internal aqueous phase is enveloped by a single lipid bilayer and the assembly is dispersed in an external aqueous phase

Unilamellar vesicles larger than 50nm are referred to as Large Unilamellar Vesicles (LUVs) while vesicles in the micrometer size range are referred to as Giant Unilamellar Vesicles (GUVs). The typical thickness of a phospholipid bilayer is in the range of 2-5nm[13]. A GUV with a diameter in the range of microns is analogous to a relatively large volume surrounded by a very thin membrane. GUVs will thus display significantly different dynamics and behavior than SUVs and LUVs. Only GUVs will be considered in this report[7] Relative sizes, surface areas and volumes are shown in figure 2.

Vesicles can, depending on the conditions of generation and the microenvironment, be either spherical or non-spherical. Although spherical geometry is generally desirable, other geometries have been studied. [33]

Thermodynamic considerations Thermodynamically, vesicle systems are generally not at equilibrium, i.e. the system diverts from a global energy minimum. The apparent system

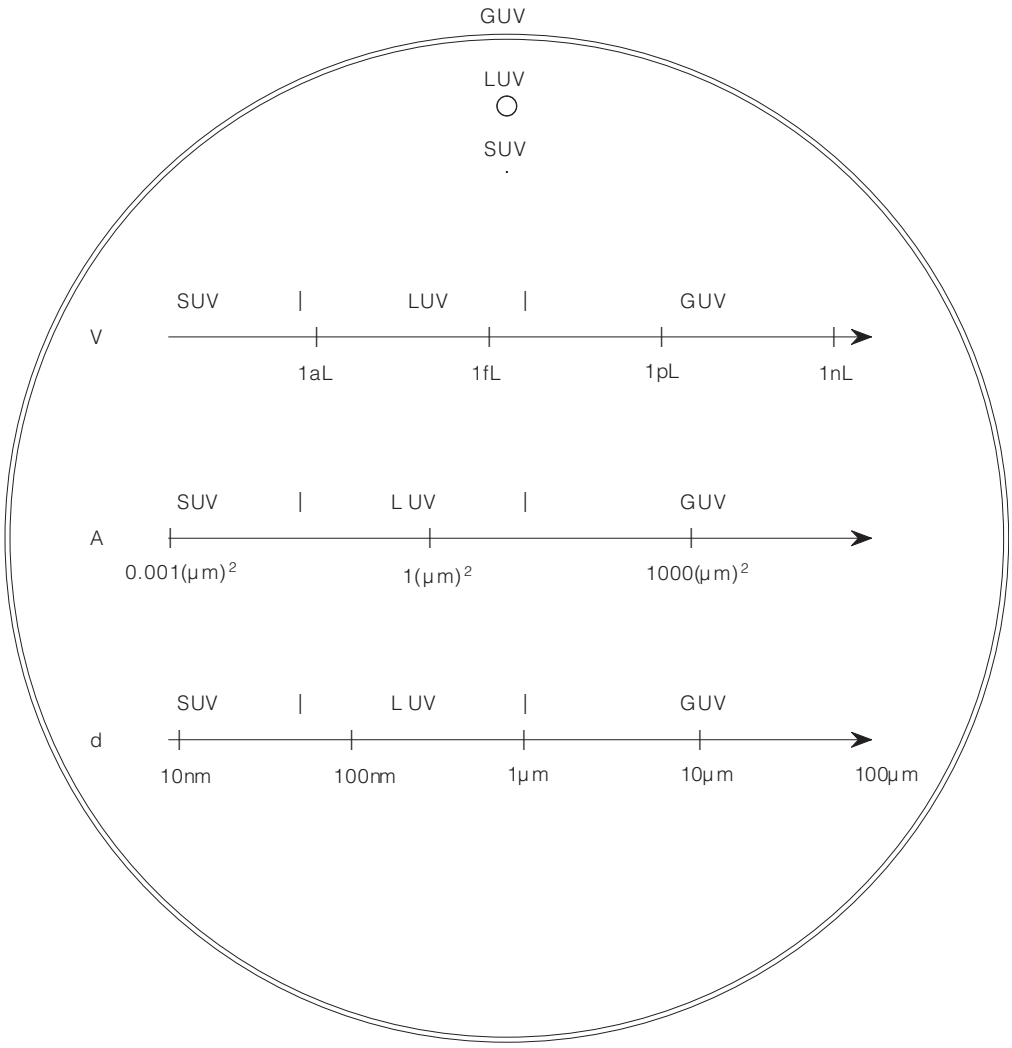

Figure 2: Characteristic diameters (d), surface areas (A) and volumes of vesicles (V). Top displays relative size of 10nm (SUV), 200nm (LUV) and 10μm (GUV)

stability indicates that the system is kinetically trapped in a local energy minimum and that the energy barrier is large enough to make the transition to thermodynamic equilibrium slow. Generally GUVs have stabilities in the range of a few hours to several months, depending on the composition of the membrane and external disturbances.

2.2 Applications of GUVs

Giant Unilamellar Vesicles (GUVs) have attracted intense attention the last decade and many potential applications have been explored. A majority of these applications use the fact that GUVs, unlike LUVs and SUVs, have sizes in the range of typical cells. GUV systems are attractive systems to model and examine dynamic biomembrane behavior. Unlike models utilizing planar membranes, GUVs systems more closely mimic their biological counterparts, e.g by allowing curvature. Many of the basic characteristics of biomembranes have been studied in GUV systems. Mechanical properties, phospholipid domain formation, budding, fission, membrane fusion as well as membrane protein integration have all been studied [33].

The relatively large size of GUVs has implications on the characteristics of the lipid membrane surface. For spherical GUVs the degree of curvature is generally small enough for the surface to be considered as flat on the molecular level. This simplifies the functionalization of the surfaces and analysis of surface phenomena.

The complex structure of GUVs allows for a wide variety of modifications. The surface can be decorated with functionalized ligands, the membrane can be modified to control transport behavior, and the interior volume allows for protein, cell and bioassay encapsulation. GUVs have been employed as biosensors in DNA microchips [2] and functionalized microwells [8].

2.2.1 Artificial cells

In 1665 the English natural philosopher Robert Hooke introduced the term *cell* to describe the smallest unit of life. Since then the cell has been at the center of biological research and scientific endeavors to understand the structure and function of living systems. The combination of cell types and cellular structures make up all living tissues.

With the last centuries of biological research, many of the components that make up cells have been thoroughly investigated. However, the dynamics of how these components interact with each other remains largely unknown. Many aspects of cells remain as black boxes to science. One fundamental realization is that the science of today generally is better at taking things apart than putting them together. The endeavor of putting a living cell together from inanimate components has been the dream of many modern scientists.

The term artificial cell was introduced in the early 20th century to describe a system that in some respect mimics the structure and/or function of a living cell. The most fundamental feature of cells is arguably compartmentalization, i.e. the subdivision of space into semi-isolated compartments that communicate through mass transfer and information transduction in a controllable fashion. GUVs represent a very appealing way to design and fabricate such systems. A GUV closely resembles a naked cell membrane and can thus be modified to mimic the semi-permeable features of cell membranes. GUVs have been extensively used for biomimetic chemistry and attempts to move towards the generation of artificial cells. These endeavors include gene and protein expression [15] [32] [21], micro bioreactors [35] [16] , cell and protein encapsulation [28], actin filament generation [27] and integrin reconstitution[26] .

Contrasting this bottom up approach, the selective elimination of genomic information to generate a minimal yet functional cell has been explored.

2.3 Membrane properties and components

2.3.1 Phospholipids

Phospholipids are amphiphilic lipids capable of arranging into lamellar bilayer structures. Phospholipids typically consists of a diglyceride, a phosphate group and small organic compound, such as a choline. Phospholipids are a major component of cell membranes.

Phospholipids display a great variety of phase and temperature dependent behavior.

In aqueous solution dispersed phospholipids can arrange in several different supramolecular arrangements. Phospholipids arrange into micelles, typically with very low Critical Micelle Concentration (CMC). The most stable arrangement for phospholipids is however the arrangement into lamellar bilayers. In this arrangement the phospholipids are positioned so that the hydrophobic ends of the phospholipids pertaining to one layer points to the hydrophobic ends of phospholipids in the other layer. This arrangement minimizes the thermodynamically unfavorable hydration of the hydrophobic molecular segments. This phenomenon, commonly referred to as the hydrophobic effect is ubiquitous in macromolecular folding and organization (of e.g. DNA and proteins).

The ability of phospholipids to arrange into lipid bilayers has implication on their temperature dependent behavior. The molecules are confined to the essentially two dimensional membrane layer and can only diffuse in the lateral directions. As a result of this phospholipid membranes display varying degrees of crystallinity depending on temperature and chemical structure.

At low temperatures the thermal motion does not overcome the van der Waals interactions between the hydrophobic tails and the phospholipids are thus forced to assume a crystalline configuration. In this state the hydrophobic tails are completely extended and the vdW interactions are maximized.

At elevated temperatures the structure of a lipid bilayer resembles a liquid crystal. The organization of the hydrophobic tails divert from that of a complete crystal and the tails are in constant motion. This allows for much higher degrees of phospholipid diffusion in the membrane and is necessary for the liquid mosaic model of cell membranes.

The temperature at which this change occurs is referred to as the phase transition temperature (T_m) and is unique for each phospholipid. The chemical structure of the phospholipid affects T_m. The presence of double bonds in the hydrophobic tail introduces kinks that limit the order of tight packing in the membrane. The vdW interactions are thus reduced along with T_m.

The coexistence of phospholipids preferring a highly ordered state (T$< T_m$) and phospholipids preferring a more disordered state (T$> T_m$) can result in phase separation within the membrane, giving rise to features protruding from the membrane surface referred to as lipid

rafts.

2.3.2 Proteins

Proteins make up an integrate part of biological membranes.

A membrane protein that bears relevance to this report is *α-hemolysin*. α-hemolysin is a cell lysing exotoxin produced by the bacteria *Staphylococcus aureus*. In solution the protein is monomeric but spontaneously inserts itself into biological membranes where it assembles into heptameric assemblies. These assemblies create pores connecting the in- and outside of the membrane leading to cell lysis *in vivo*. α-hemolysin is highly specific and only integrates into true phospholipid bilayers. This feature has made it the golden standard of proving the presence of artificially generated phospholipid bilayers in lipid vesicles. [18] [16] [24]

2.3.3 Membrane permeability

The ability of a semi-permeable membrane to allow the transport of a solvent across the membrane interface is described by its permeability to that solvent. For most applications involving vesicles in general and for this report in particular the solvent is water and it is thus the membranes ability to allow or obstruct the transport of water that is of interest. The density of the membrane packing as well as the mobility of the membrane components and degree of hydrophobic barrier present in the membrane all affect the extent of permeability. A common way to examine the permeability of a phospholipid membrane is to subject it to an osmotic pressure shock. An osmotic pressures shock involves the drastic increase (or decrease) of the osmolarity of the external solution. The osmolarity can be increased by adding a solute that cannot move though the membrane (often sucrose) to the external solution. The difference in solute concentration and the resulting osmotic pressure forces water molecules to move through the membrane from the internal solution to the external. The transport ceases when the two solutions are in equilibrium once again. The loss of water result in drastic shrinking and sometimes collapse of the vesicle.

The permeability of a vesicle can be extracted from its response to an osmotic pressure shock.

The flux of water across a semipermeable membrane can be expressed by equation 1.[34]

$$J = \frac{\dot{n}}{A} = -P\Delta c[mol/sm^2] \tag{1}$$

$$\dot{V} = \dot{n}\alpha, \dot{V} = [chainrule] = A\dot{r} \tag{2}$$

$$\dot{r} = -\alpha P\Delta c \tag{3}$$

Where $\dot{n}$ is the rate of molar transport across the membrane, A the characteristic surface area of the membrane, P membrane permeability, Δc the difference in solute concentration

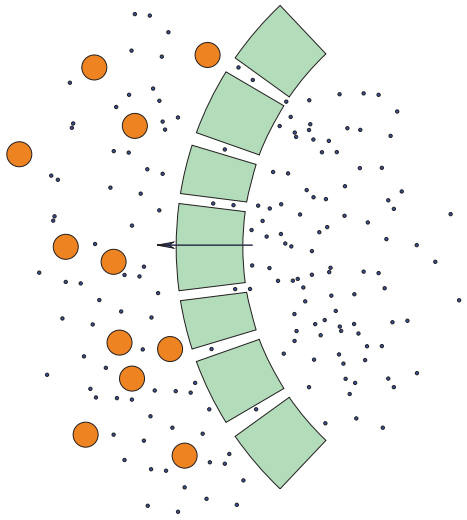

Figure 3: Phospholipid bilayers are semipermeable and allow transport of water molecules between the internal and external aqueous medium. Illustration shows vesicle response to an increase in osmolarity of the external solution

across the membrane, $\dot{r}$ is the rate of change in vesicle radius, α the molar volume of water and $\dot{V}$ the rate of volumetric change. Phospholipid vesicles normally have permeabilities in the range of 15-150 μm/s. It is commonly assumed that trapped solvent leads to significantly reduced permeabilities. [18]

3 Vesicle generation

The fact that vesicle systems generally represent kinetically trapped states rather than thermodynamic equilibrium has implications on the process of vesicle generation . Since vesicle systems generally only represent a local thermodynamic energy minimum, not only the composition of the membrane influences the final result but also the way that the system is prepared. In other words, a combination of phospholipids known to form lamellar structures at equilibrium, e.g. as a flat membrane in aqueous solution, does not necessarily form unilamellar vesicles with an arbitrary generation method. These considerations increase the complexity of vesicle generation. [33]

Traditional methods for analyzing phospholipid systems often include creation of equilibrium state phase diagrams. This type of analysis is therefore generally of limited use for vesicle generation.

3.1 Existing methods

A comprehensive review of GUV generation was recently published.[33] Here follows a short summary of the most common techniques used today. For more in depth information the reader is referred to this review.

3.1.1 Gentle hydration and electroswelling

The first method to generate GUVs was published by Reves and Dowben in 1969 and since then a diverse range of generation techniques have been developed.

The method described by Reves and Dowben involved the careful hydration of a dried phospholipid film deposited on a glass surface though evaporation of a volatile solvent. The process was very delicate and even the smallest disturbance during the generation resulted in significantly reduced yields. When disturbed, the process produced predominantly smaller multilamellar vesicles.[20] The modernized version of this technique is referred to as spontaneous swelling or gentle hydration and works particularly well with phospholipids with charged head groups. It is important to note that the method only works at temperatures above Tm. In order to give vesicles with a narrower size distribution, surface patterning has been successfully used. [33]

A variation on this theme is the technique referred to as electroswelling. Here, an applied AC electric field helps in the generation process. In recent years the technique has been modified so that the lipid film deposited in the surface is prepared from SUVs and LUVs rather than unorganized phospholipids. The lipid film can thus not be completely dried in the deposition step, in order to retain these structures.

The original electroswelling technique is, unlike the gentle hydration technique, disfavored for lipid compositions with mainly charged lipids. Interestingly enough, the electroswelling method results in protrusions in the membrane structure. The elongated features can be stable for several hours and can thus be a nuisance for applications that require exclusively spherical vesicles. Some concern has also been raised about the possibility of oxidation of the lipids involved and other sensitive components due to the presence of the electrical field. Furthermore, the vesicles remain connected to the surface from which they where spawned and will thus likely behave differently from free vesicles.[33] Electroswelling requires the aqueous medium to have minimal ionic strength, thus making the use of most common buffers used for proteins and cells impossible. [36]

Both the gentle hydration and the electroswelling technique are generally unsuitable for encapsulation of molecules within the vesicles, encapsulation experiment generally produce low yields. Encapsulation can however be achieved through microinjection directly into the vesicles, a very laborious process. Furthermore the vesicles are already filled with the buffer used and thus very limited amounts of extra fluid can be added. Despite of these drawbacks the electroswelling method is currently the most widely used technique for GUV generation. [33]

3.1.2 Water-in-oil emulsion transfer method

GUVs can also be prepared from emulsions stabilized by phospholipids. In the water-in-oil emulsion transfer method, aqueous microdroplets are prepared in an oil phase containing an excess of solubilized phospholipids. The phospholipids will spontaneously form a lipid monolayer in the interface between the two phases and thus a stabilized water-in-oil emulsion is formed.

The oil phase is then macroscopically brought into contact with an aqueous phase, resulting in the spontaneous formation of a lipid monolayer separating the two bulk phases. The phases are chosen so that the oil phase naturally resides on top of the water phase. The microdroplets will, due to gravity, transfer to the aqueous phase and doing so, a lipid bilayer will be formed as the droplet crosses the interface between the phases. If gravity alone isn't enough to make the droplets transfer within a reasonable timeframe, centrifugation can be employed to speed up the procedure. The lipid bilayer is thus created in two independent steps and the creation of asymmetric bilayer appears therefore to be possible.

The method is dependent on the generation of aqueous microdroplets with satisfying control of size and chemical composition. The size of the droplets generated initially determine the size of the vesicles. Residues of the oil phase present in the bilayer after transfer is a possible drawback to this technique. [33]

3.1.3 Methods involving microfabrication

As stated earlier the successful generation of vesicles is highly dependent on the exact manner of how the vesicles are generated. Here follows a short discussion on some of the methods involving microfabrication that have been proposed for vesicle generation.

T-junction Ota et al. employed a T-junction like layout to generate lipid vesicles. A microfluidic device with multiple modified T-junctions was sequentially primed with water and phospholipid containing oil. This creates a layer of phospholipid containing oil in the T-junction. Then the pressure in the water containing side channel orthogonal to the main channel was increased through the action of a laser, a flow is created from the side channel into the main channel. As the water flows into the main channel, the lipid membrane folds around the emerging droplet and an unilammellar vesicle is created.[18] A major limitation of this methods is that the lipid phase is not replenished and will thus run out after a period of device use. The vesicle size appears to be tunable in the range between 11 and 14μm, which can be unsatisfactory for applications requiring a wider range of tuning.

Jetting of planar membrane Stachowiak et al. described a method for generating unilamellar vesicles by jetting of aqueous flow through a planar lipid membrane extended between two circular microfluidic compartments. [24] As with the case of T-junction generated vesicles, the lipid layer is not replenished. Furthermore, the device generated vesicles in sizes

around 200μm, which is more than an order of magnitude larger than a typical cell and can thus be assumed to be less useful for biological applications. No indication as to how the vesicles can then be efficiently extracted and strategies to increase the throughput of the system are given.

Microfluidic double emulsions Shum et al. described a method for generating vesicles from double emulsion templates. In their microfluidic device double emulsions are formed by dispersing aqueous droplets in a volatile organic phase (toluene and chloroform). The W/O (water-in-oil) emulsion is then, almost instantly dispersed in an external aqueous phase. The result is a W/O/W (water-in-oil-in-water) double emulsion. The volatility of the organic phase allows it to evaporate through the external aqueous phase, resulting in the formation of a lipid bilayer around the internal aqueous phase, consisting of the phospholipids that were originally dispersed in the organic phase.[23] This method offers a considerable number of advantages compared to the methods discussed above. The method can take full advantage of the high throughput characteristics of microfluidic droplet generation, allowing generation rates of about 500Hz. Since the lipid membrane is continuously generated from a bulk organic phase it is replenished and does not run out. Although the double emulsions described by Shum et al. were relatively large (40μm) it is very likely that smaller double emulsions could be generated with a similar setup. A major drawback is however the use of volatile organic compounds, which are both complicated to work with in a standard microfluidic setup and potentially harmful to biological samples. PDMS is known to swell extensively in the presence of organic solvents, resulting in changed characteristics of the device channels.

4 Microfluidic generation of vesicles

With the existing methods in mind, desirable features for the vesicle generation method to be developed could be summarized.
The method should allow:

- Vesicle generation in the size range of typical cells
- Vesicle generation in standard microfluidic devices, not requiring true 3D elements
- Tunable size, adaptable for different applications
- High generation throughput
- Use of only non-aggressive organic solvents or other biocompatible components
- Tailorable internal composition in the generation step, no post generation modification needed

4.1 Microfluidics

4.2 Laminar flow

Reynolds number Re is normally used to characterize the flow of a fluid in a channel. Reynolds number is a dimensionless number expressing the ratio between inertial and viscous forces in a single continuously flowing liquid, see equation 4, where ρ is the density of the liquid, D_h the hydraulic diameter, v the liquid velocity and μ the liquid viscosity.

$$Re = \frac{\rho D_h v}{\mu} \tag{4}$$

At low Re values the viscous forces dominate and the flow follows strictly laminar characteristics, with a well defined flow profile and minimal convection. Transition to turbulent flow normally occurs at Re = 1000-2000 in micro channels. Water flowing at a flow rate of 10μl/min in a channel with a hydraulic diameter of 50μm gives a Reynolds number of approximately 4. It is therefore safe to conclude that all microfluidic flow in this report is strictly laminar.

The pressure drop Δp through a channel containing a laminar flowing liquid is described by the Hagen-Poiseuille equation, see equation 5, where μ is the liquid viscosity, L the length of the channel, Q the volumetric flow in the channel ($Q = vA$) and r the hydraulic radius of the channel.

$$\Delta p = \frac{8\mu L Q}{\pi r^4} \tag{5}$$

For a channel with circular cross section the hydraulic diameter is equal to the physical diameter of the cross section. For other geometries, such as square and parabolic channels common in microfluidic devices, the hydraulic diameter can be calculated using 6, where A is the cross sectional area and P_{wet} the wetted perimeter of the channel.[14]

$$D_h = \frac{4A}{P_{wet}} \tag{6}$$

4.3 Droplet microfluidics

4.3.1 Droplet generation

As discussed above flow in micro-channels is typically purely laminar and well described by the governing equations for most liquids. The presence of a second phase increases the complexity of the system considerably as well as the presence of a fluid velocity. The behavior of the system will be determined by the competition between interfacial, viscous, inertial and to a smaller extent gravitational forces. Through dimension analysis this interplay can be described by dimensionless numbers comparing the magnitude of one influence to another. [6]

The ratio between gravitational and interfacial influence in a multi-phase system is given by the *Bond number, Bo*, see equation 7, where $\Delta\rho$ is the density difference between he two

liquid phases, g the gravitational acceleration, D_h the hydraulic diameter of the channel and γ the surface tension.

$$Bo \equiv \frac{\Delta \rho g D_h^2}{\gamma} \tag{7}$$

For microfluidic systems Bo $\ll 1$ indicating that minimal influence of gravity can be assumed. [6]

In static conditions with neglectable influence for gravity two phases are in equilibrium if they have a uniform pressure distribution and the pressure of the phases only differ by the capillary pressure described by the Young-Laplace equation, see equation 8, where γ is the surface or interfacial tension and r the local curvature of the system. [6]

$$\Delta P_{Y-L} = \gamma r \tag{8}$$

The pressure difference ΔP_{Y-L} it thus influenced by both chemical composition (e.g. presence of surfactants) as well as the physical dimensions of the system. ΔP_{YL} is of considerable magnitude in micro and nano channels due to the small typical length scale and degree or curvature. [6]

The laminar characteristics of flow in microchannels, combined with the domination of surface forces leads to the creation of highly uniform interfaces and boundaries.

The degree of contact between the phases and the channel walls is defined by the contact angle created in the three-phase region where the fluid interface meets the channel wall interface. Assuming that none of the present phases form a film that adsorbs to the channel wall, the contact angle can be calculated by the Young equation, see equation 9, which relates it to the surface energies of the interfaces.

$$\gamma_{l_1 l_2} \cos(\theta) = \gamma_{l_1 s} - \gamma_{l_2 s} \tag{9}$$

The contact angle determines the wetting ability of a liquid on a specific surface. Wetting liquids have small contact angles while non-wetting liquids have contact angles $\approx 180^o$.[6]

The wetting characteristics of a system is of utmost importance for droplet generation. Ideally the phase that is to be dispersed into the continuous phase should be completely non-wetting. If the dispersed phase has a tendency to wet the channel walls the interface in the droplet generation junction will be distorted and lead to the inverse scenario where droplets are formed broken off from the continuos phase. The wetting characteristics of a fluid can be modified to suit the application by chemically altering the composition or structure of the channel walls (e.g though polyvinyl alcohol treatment).

In the case of flow focusing devices, droplet generation results from the competition of opposing forces and the occurrence of system instabilities. The relative velocity of the two phases induces a viscous shear on the liquid interface whereas capillary stress is created by the interfacial tension of the system. While viscous stress strives to stretch and elongate the interface, capillary stresses strive to minimize the area of contact between the phases.

This interaction is described by the *Capillary number, Ca.* Equation 10 defines Ca for a spherical droplet of diameter D, suspended in a liquid with the viscosity μ, magnitude of the local fluid velocity v and interfacial tension γ. [3] [6] [30]

$$Ca \equiv \frac{\mu v D}{\gamma} \tag{10}$$

Viscous forces are volume based and interfacial forces are bases on area. Following the discussion above, droplets in micro-channels typically experience low Ca numbers. At Ca=1 viscous forces can still deform the interface and cause droplet break-off. Furthermore, at this condition (Ca=1) the generated droplet diameter is directly dependent on the flow rate of the shearing liquid, a higher flow rate will result in a smaller droplet. Using simple approximations the droplet diameter can be estimated with equation 11, where $D_{channel}$ is the hydraulic diameter of the channel. [3]

$$D \sim \frac{\gamma D_{channel}^3}{\mu} \tag{11}$$

For droplets with diameters comparable to the width of the channel hydrodynamic forces induced by the presence of channel walls start to interfere and limit the use of equation 11 and the flow rate of the shearing liquid is less influential on droplet diameter. Surfactants can be added to a system to decrease the interfacial tension, leading to an increase in Ca and in the likelihood of droplet break-off. Following droplet generation, surface tension serves to relax the droplet to a more spherical shape. [3]

Considerations of the timescales involved in the process of droplet generation has shown that droplet generation is dominated by the capillary pinch-off time rather than the time it takes to deliver enough volume to form a droplet. [3]

In order to break the interface between the phases and create droplets, some kind of transient instability is necessary. Classically the capillary instabilities resulting in droplet break-off from sheared, unbounded, cylindrical interfaces in flow focusing devices are referred to as Rayleigh-Plateau instabilities and result in the formation of monodisperse droplets. [6] Rayleigh-Plateau instabilities are caused by interfacial tension and the drive to minimize interfacial area.

Flow focusing devices generally display three distinct droplet generation regimes. At low flow rates the droplets typically break off beyond the point of the actual junction, with typical sizes larger than the junction orifice. This regime is referred to as the dripping regime. At intermediate flow rates the droplet break off occurs within the junction orifice. The tip of the interface typically retracts after each generation event. At high flow rates the interface appears to be fixed in position relative to the orifice. The continuous phase forces the dispersed phase to take on a jet-like configuration where the thin thread of dispersed phase is broken of into small droplets beyond the point of the orifice. This regime typically produces satellite droplets and relatively polydisperse populations and is referred to as the jetting regime.[22]

The transition from the dripping to the jetting regime can be explained by considering the characteristic timescales involved. There is a characteristic pinch off time (t_{pinch}) associated to the propagation of the Rayleigh-Plateau instability. However, the Rayleigh-Plateu instability can only occur when the jet of dispersed fluids has grown to a certain size. The growth of the jet can be expressed in terms of a characteristic growth time(t_{growth}). In the dripping regime $t_{pinch} < t_{growth}$ and droplets are created as soon as the jet is large enough to sustain the instability. In the jetting regime $t_{pinch} > t_{growth}$ and the jet grows quicker than the Rayleigh-Plateau instability can pinch off droplets. The Capillary number can be expressed as the fraction between the two time scale, see equation 12 but gives the expression in equation 10 after mathematical treatment. The transition from dripping to jetting generally occurs around $Ca \sim 1$. [31]

$$Ca \equiv \frac{t_{pinch}}{t_{growth}} = \frac{\mu_e Q_{disp}}{\gamma R_{jet}^2} = \frac{\mu v D}{\gamma} \tag{12}$$

Through equation 12 Ca connects the timescales to the physical parameters of the system. The transition from a dripping regime to a jetting regime occurs when the viscous stresses imposed by the external phase suppresses the Rayleigh-Plateau instability.

4.3.2 Double emulsion generation

One-step double emulsion generation in a microfluidic channel has been shown. Utada *et al.* reported the existence of two characteristic regimes, a dripping and a jetting regime analogous to the single emulsion counterparts. The double emulsions can be designed to have one or more inner droplets. The encapsulation of a single inner droplet per double emulsion occurs when both the dispersed phases are in the regime of generation and break off occurs at the same time for both phases. As reported for single emulsion it is the viscous stress induced by the external phase that determined the mode of generation. Dripping occurs at lover flow rates of the external phase and the jetting regime is reached when the external flow rate is increased. Utada *et al.* showed that characteristics of droplet generation largely applies for double emulsions. [31]

4.4 Vesicle generation through solvent extraction

4.5 Pumping

There are two main ways of generating flow in microfluidic devices. Most widely used method is to use a syringe pump with a set volumetric flow rate (displacement driven flow). Alternatively a pressure can be imposed at the device inlets by using a pressure regulator and a gas pressure source (pressure driven flow).

The two methods are fundamentally different in which parameters they allow the user to control. Displacement driven flow allows the user to set the volumetric flow rate but allows

no control of the pressure generated by the pump. It is therefore common that the pressure in the channels can vary heavily and pressure spikes are common during device setup. The flow from a syringe pump is generated by a stepper motor that takes discrete steps at a changeable rate. The flow will therefore never be completely continuous and some pressure variations are commonly observed.

Pressure driven flow allows the control of inlet pressure and volumetric flow is thus only indirectly controlled. Since a constant pressure can be applied to the inlets of a device the resulting flow will be truly continuous. However, since the flow rate cannot be easily determined the data analysis from such experiments is often more complicated than data analysis from experiments using displacement driven flow. Furthermore it is harder to transfer experimental settings between devices with different design because the channel flow resistance generally is unknown. It is also hard to compare flow rates in channels with different inlets and channel lengths. However, pressure driven flow is much more suitable for delicate processes than displacement driven flow, since no pressure spikes occur. Pressure driven flow also responds much quicker to a change in settings and flow profiles tend to stabilize more rapidly, especially during start up.

5 Dielectrophoresis, DEP

In an inhomogeneous electric field a polarizable particle will be subjected to a Coulomb force that is independent of particle charge and has a non-zero time average even in AC fields. This effect is referred to as dielectrophoresis.

5.1 DEP of vesicles

DEP is attractive as a way to manipulate vesicles for a number of reasons:

- DEP is non-invasive, it requires no special probe or chemical modification of the target
- DEP is fully reversible, allowing transient and sequential manipulation without affecting the vesicle chemistry
- DEP is both size and chemistry selective and offers many possible criteria for manipulation
- DEP allows complex manipulation
- DEP devices can be fabricated using standard photo and soft lithography protocols
- DEP directly interfaces with electronic and programmable controlling mechanisms, which allows for automatization

DEP of vesicles of varying sizes has been modeled and described previously [5][10][25][4] In order to determine the chemical and physical parameters controlling the DEP response of living cells, vesicle have been used as model systems. Vesicles can readily be tailored to

capture different aspects of cellular DEP response.[25] Korlach *et al.* used electric field traps to trap and deform vesicles.

5.2 Theory

Consider a dielectric, isotropic, homogeneous particle in a homogeneous electrical field suspended in space. The electric field will cause the particle to polarize and thus create a positive charge in one end of the particle paired with an equal negative charge in the opposite end. The Coulomb forces induced by these charges are thus equal and opposite, resulting in a zero net Coulomb force on the particle.

If the electrical field is inhomogenous, thus stronger in one end of the particle, the induced charges will have different magnitudes, resulting in the creation of a dipole. The resulting Coulomb force will be non-zero. This will result in a net migration of the particle towards the region with a stronger field.

For a particle in a dielectric medium the analysis is more complex. A dielectric medium will polarize as well as the particle suspended in it, resulting in the formation of Maxwell Wagner interfacial charges. If the particle polarizes more than the surrounding medium the particle will be subjected to a force towards a higher field region. If the particle polarizes less than the surrounding medium the resulting force will point towards a lower field region. The movement of a particle towards a higher field strength is referred to as positive dielectrophoresis, whereas the opposite is referred to as negative electrophoresis.

As a result of the above considerations, the DEP force is independent of the polarity of the electric field and only dependent on the field strength (and phase). Thus, the DEP has a non-zero average regardless if DC or AC electric fields are used.

Mathematically, the DEP force $\overrightarrow{F}_{DEP}$ is dependent on the scalar product of the induced dipole moment and the electrical field, see equation 13 where $\overrightarrow{p}$ is the induced dipole moment and $\overrightarrow{E}_0^*$ is the complex conjugate of the electrical field.[1]

$$\overrightarrow{F}_{DEP} = \frac{1}{2}\Re(\overrightarrow{p}(\omega) \cdot \nabla \overrightarrow{E}_0^*) \tag{13}$$

The dipole moment in turn is dependent on the degree of polarization, given as a function of the first order polarization coefficient and the electrical field in equation 14.

$$\overrightarrow{p}(\omega) = 4\pi\widetilde{\epsilon}_e r^3 f_{CM}(\omega)\overrightarrow{E}_0 \tag{14}$$

The polarization coefficient, commonly referred to as the Clausius-Mosotti factor f_{CM}, describes the permittivity of the particle relative to the surrounding medium, see equation 15. In other words f_{CM} describes how different the permittivity of the particle is compared to the medium.

$$\widetilde{f_{CM}} = \frac{\widetilde{\epsilon}_p - \widetilde{\epsilon}_e}{\widetilde{\epsilon}_p + 2\widetilde{\epsilon}_e} \tag{15}$$

A material's polarizability can be described by its complex permittivity. The complex permittivity takes into account the static permittivity as well as the frequency dependent permittivity influenced by a material's conductivity.

$$\widetilde{\epsilon} = \epsilon - \frac{\sigma i}{\omega} \tag{16}$$

From the above equations it is evident that both $\widetilde{\epsilon}$ and $\widetilde{f_{CM}}$ are complex quantities. $\widetilde{f_{CM}}$ contains much of the information needed to determine the behavior of the system. The magnitude of $\widetilde{f_{CM}}$ is dependent on the magnitude of the induced Maxwell-Wagner charges. $\Re\left[f_{CM}\right]$ describes the part of the dipole moment that is in parallel with the electric field and $\Im\left[f_{CM}\right]$ describes the part orthogonal to it. Thus $\Re\left[f_{CM}\right]$ is relevant for dielectrophoresis while $\Im\left[f_{CM}\right]$ determines the extent of electrorotation. The upper limit of $\Re\left[f_{CM}\right]$ is 1 and indicates a maximum in positive DEP, whereas the minimum $-\frac{1}{2}$ indicated a maximum in negative DEP.

The time averaged DEP force for a particle suspended in a dielectric medium subjected to a AC inhomogeneous real electric field is described by equation 17.

$$< \overrightarrow{F}_{DEP} >= \pi \widetilde{\epsilon_e} r^3 Re\left[f_{CM}\right] \nabla |E_{rms}|^2 \tag{17}$$

The term $\nabla |E_{rms}|^2_{trap}$ gives the directions in the which the density of the electric field lines increases and thus gives the direction of positive DEP. Equation 16 describes the permittivity of a isotropic homogenous particle. This is not an adequate proximation for a vesicle. The permittivity used must take into account the contributions of the membrane as well as the aqueous core.[9]

A multi-shell model, based on Maxwell-Wanger theory has been proposed to approximate the resulting permittivity in therms of dielectric properties of the shell layers, see 18, where γ is the ratio of the outer and inner radius of the shell, $\widetilde{\epsilon_m}$ is the permittivity of the membrane and $\widetilde{\epsilon_i}$ is the permittivity of the internal solution. [5]

$$\widetilde{\epsilon_p} = \widetilde{\epsilon_m} \frac{\gamma^3 + 2\frac{\widetilde{\epsilon_i} - \widetilde{\epsilon_m}}{\widetilde{\epsilon_i} + 2\widetilde{\epsilon_m}}}{\gamma^3 - \frac{\widetilde{\epsilon_i} - \widetilde{\epsilon_m}}{\widetilde{\epsilon_i} + 2\widetilde{\epsilon_m}}} \tag{18}$$

From the above theoretical considerations is is obvious that DEP depends on the properties of the internal phase as well as the membrane. Desai *et al.* created Electrically Addressable Vesicles by modifying these properties and linking them to the DEP response of the vesicle.[4]

The effect of DEP has a typical size range. The lower limit ($\approx 1\mu$m) is set by Brownian motion dominating over the DEP force, while the upper limit ($\approx 1000\mu$m) is set by the emerging effects of gravity.[1]

5.3 DEP trapping

As discussed above a vesicle can, under certain conditions, be subjected to positive DEP in an inhomogenous electric field. This ability can be used to trap vesicles. Ignoring gravity and

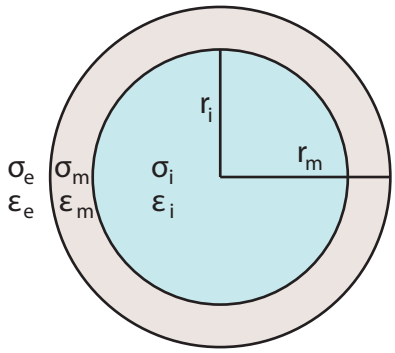

Figure 4: Shell model for the complex permittivity of a vesicle

buoyancy, the criteria for DEP trapping is that the DEP force must overcome the viscous drag on the vesicle, induced by the flow of the medium. At low reynolds numbers the drag on a particle suspended in a continuous viscous medium is given by *Stokes' law*, see equation 19, where μ is the viscosity of the surrounding medium, r is the particle radius and v_m the settling velocity of the particle.[14]

$$F_{stokes} = -6\pi\mu r \overrightarrow{v}_m \tag{19}$$

A force equilibrium between the DEP force and Stokes drag force gives rise to an equation describing DEP trapping.

$$\nabla|E_{rms}|^2_{trap} = \frac{-6\mu \overrightarrow{v}_m}{\epsilon_m r^2 Re\,[f_{CM}]} \tag{20}$$

Using fundamental considerations of the relation between the electric field and the applied electric voltage ($E = -\nabla\phi$) it is evident that an increased voltage leads to an increase of the term $\nabla|E_{rms}|^2_{trap}$. Thus a trapping voltage U_{trap} is associated with each particle size and velocity. If $Re\,[f_{CM}]$ can be assumed to be equal to 1 independently of r, a good approximation for vesicles in the size range of 10-30 μm the trapping voltage is proportional to $\frac{1}{r^2}$. This indicates that larger particles can be trapped at lower voltages than smaller particles. Thus condition where only a subpopulation of a heterogenous vesicle population are trapped should exist.

Part II
Materials and Methods

6 Device fabrication

6.1 Silicon wafers

Silicon wafers were used to make molds for soft lithography. Silicon wafer orientation and doping is of no importance in soft lithography.

6.2 Photoresists

Photoresists are light sensitive compounds used to generate designable patterns though photolithography. There are two main categories of photoresists, positive photoresists and negative photoresists. Positive photoresists are compounds that are made mobile by UV radiation, resulting in a pattern that is the same as that of the mask used (i.e. *positive*) after development. Negative photoresists are immobilized by UV radiation and generate patterns that are opposite that of the mask (i.e. *negative*).

SU8 SU8 is an epoxy-based negative photoresist. SU8 was developed by IBM for the semi conductor industry but has gained great popularity in the microfluidics/MEMS community due to its ability to sustain high aspect ratios and thick features. Feature heights of 2mm at an aspect ratio of 20 have been reported. SU8 has an absorbance maximum at 365nm and exposure leads to cross-linking of the resist molecules. SU8 has good mechanical properties and can be used directly as structural and mechanical components. There are many series of SU8 with different viscosities, optimized for different aspect ratios and feature heights. [12]

AZ4562 AZ4562 is a series of positive photoresists. AZ resist can be spin coated to thicknesses of about 100μm. Az photoresist has good adhesive capabilities and is suitable for highly resolved pattering. AZ4562 is often used to pattern metals deposited on glass.[14]

6.3 Masks

Masks for photolithography were designed using AutoCAD software. The masks were printed with high resolution printing onto transparency sheets on commission by CAD/Art Services, Poway, CA. The company guarantees resolution down to 10 μm features.

6.4 Soft lithography

Molds for soft lithography were prepared from [1.0.0] Si-wafers and SU8 photoresist using standard methods of photolithography, see figure 5. Prior to mold fabrication SI wafers were thoroughly cleaned. RCA1 cleaning was used to remove all deposited organic compounds and HF cleaning was used to remove any native SiO_2.

SU8-50 was deposited on the wafers by spin coating. The spin rate was modified to give the desired feature height. A spin rate of 3000rpm gave a 50 μm standard height for all wafers. The wafters were soft baked at 95^{o}C for 7 minutes. Wafers with deposited SU8 were flood exposed with 365nm UV radiation ($17mW/cm^2$) for 13s through proximity masks containing device designs. Post exposure bake was set to 6 minutes at 95^o C.

After development of the SU8 the wafers were hard baked at 175^oC for 2h to remove any cracks, smoothen and shrink feature sizes. The wafers were silanized twice with TMCS to minimize the adhesion of PDMS to the SU8 features.

6.5 PDMS molding

Poly dimethyl siloxane (PDMS) polymer was used to create all devises described in this report. PDMS is an elastomeric polymer with high optical transparency and low autofluorescence. Native PDMS has a low interfacial free energy, resulting in poor water wettability and good oil wettability. Despite PDMS:s enormous popularity as a material for rapid prototyping and soft lithography it suffers from a number of limitations. PDMS is highly elastomeric and readily deforms as a result of pressure changes or other mechanical strains. PDMS also swells considerably by absorbing many common organic solvents, leading to transient changes in channel dimensions. The elastomeric properties also limit the maximum aspect ratio, paring often leads to collapse of high and thin features. In very wide channels the channel roof is likely to collapse due to the lack of mechanical support. An aspect ratio between 0.2 and 2 is recommended for most PDMS applications.[14]

6.6 Device assembly

Cured PDMS containing the device designs was cut out from the silicon/SU8 molds and bonded to naked glass slides or PDMS coated slides using an oxygen plasma, see figure 6. The oxygen plasma operates at a pressure of 300mTorr for 2.5 minutes to activate the PDMS and glass surfaces. Activation occurs by oxidizing the surfaces and replacing methyl groups with hydroxyl groups that can participate in the formation of silanol bonds between the glass slide surface and the device containing PDMS. The formed bond is thus covalent and heat treatment increases bonding strength by increasing the yield and rate of the condensation reaction. Schematic of the device fabrication and assembly can be seen in figure 5. Some small features in the device designs, such as the orifice width were observed to have increased in size

in the assembled devices. This is most likely a result of enlargement in the pattern transfer processes during photo and soft lithography.

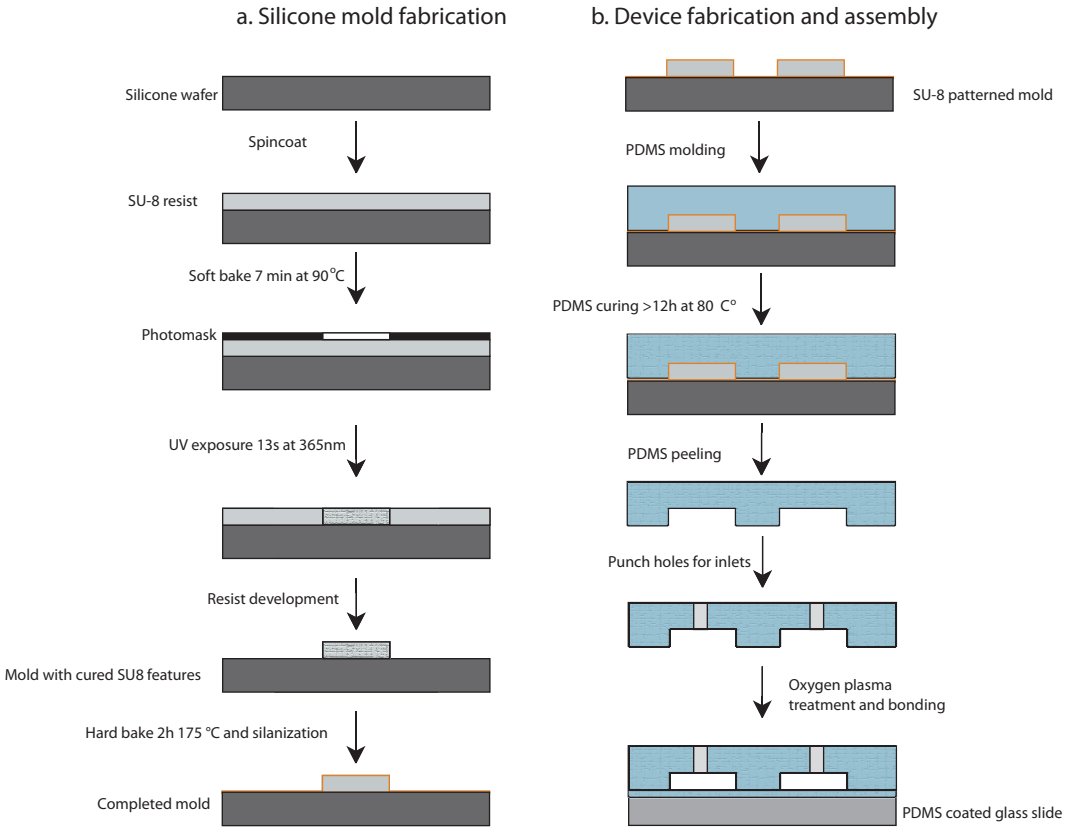

Figure 5: (a) SU8-silicon mold fabrication, (b) PDMS device fabrication and assembly

6.7 Surface treatment

To taylor the wetting properties of the PDMS channels surface modification through passive deposition was used. Polyvinyl alcohol (PVA) is a hydrophilic polymer that readily adsorbs to PDMS surfaces, resulting in a drastic change in the hydrophilicity of the surface. Treated surfaces are readily wetted by aqueous phases but not by most organic solvents.[11] A 0.5% PVA in water solution was flowed through the channel intended for treatment by applying a small solution droplet to the channel inlet and sucking it though the device by applying a light vacuum to the outlet. The PVA layer is fixed by treating the device for 15 minutes at 120^{o}C. PVA treatment proved to be a very important yet sensitive part of device fabrication. The

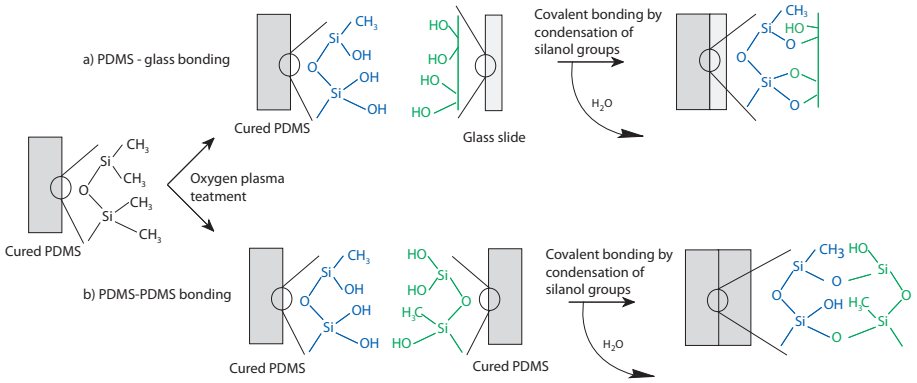

Figure 6: Oxygen plasma bonding of (a) PDMS-glass and (b) PDMS-PDMS though surface activation and silanol condensation

slightest deposition of PVA in the device parts intended to the hydrophobic generally resulted in complete device malfunction.

6.8 Gold electrodes

Titanium and gold layers was consecutively deposited onto glass slides using E-beam evaporation deposition. A 100nm gold layer was deposited on a 25nm titanium adhesion layer. The slides where spin coated with AZ resist and thereafter flood exposed with 365nm UV radiation through proximity masks containing the electrode designs. The AZ resist was developed followed by etching of the gold and titanium layers. After development the slides were bonded to wide channeled PDMS devices. Wires were connected to the electrodes with silver epoxy.

7 Device designs

7.1 Junction type N

Teh *et al.* designed devices generating double emulsions in two consecutive flow focusing droplet generation junctions. In the first junction a W/O single emulsion is generated followed by the dispersion of the W/O emulsion into another aqueous phase, resulting in a W/O/W double emulsion. This general type of device design served as the starting point for the device development that is described in this report.

7.2 Junction type A

In an attempt to circumvent some of the problems associated with the N type junctions novel approaches to double emulsion generation were pursued. Instead of splitting the double emul-

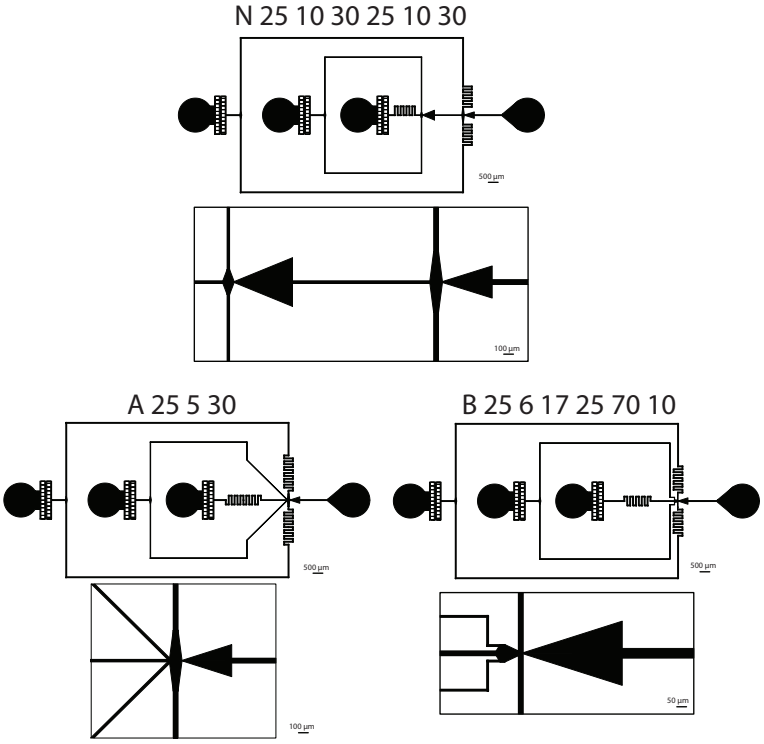

Figure 7: Typical designs of the three junction types used

sion generation into two consecutive steps a design where the double emulsions are generated in a single junctions was developed. This category of device designs are here referred to as A type junctions, see figure 7.

7.3 Junction type B

A third junction design is proposed in this report, referred to as a B type junction. In this junction type the oil and internal phase are allowed to co-flow in a triangular channel section leading up to the actual generation junction, see figure 7.

8 Oil phase components

Oleic acid was used as bulk organic phase in all experiments. Oleic acid is a monounsaturated omega-9 fatty acid, see figure 9 for structure. Oleic acid is immiscible in water and soluble in alcohols, such as methanol and ethanol. Phospholipids are readily dispersible in oleic acid.

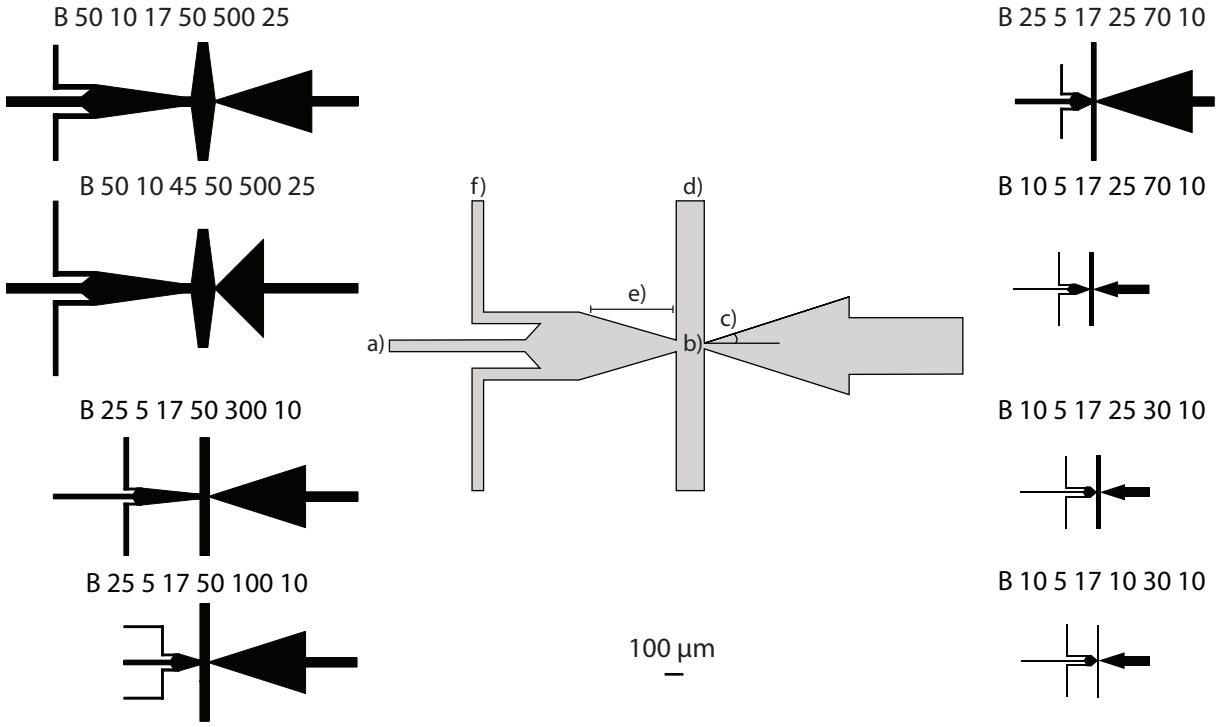

Figure 8: B type junction designs. Numbers indicate characteristic distance (μm) of (a) internal phase channel, (b) junction orifice, (c) outlet angle, (d) external phase channel, (e) co-flow region and (f) oil phase channel.

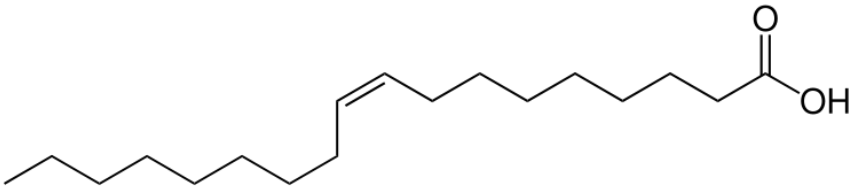

Figure 9: Chemical structure of oleic acid

Oleic acid	
Chemical formula	$C_{18}H_{34}O_2$
Molecular weight	282.47 g/mol
Density	0.895 g/ml
Viscosity	27.64 (@25^oC)
pKa	5.02

8.1 Phospholipids

The phospholipid 1,2-dioleoyl-sn-glycero-3-phosphocholine (DOPC) was used to create vesicles in all experiments. DOPC has two monounsaturated fatty acids and a choline head group, see figure 10 for structure. The unsaturation of the fatty acid chains introduce kinks in spacial configuration of the molecule making tight packing of the phospholipid in a liquid crystal inefficient, resulting in a very low transition temperature (-19^oC). The permeability of a DOPC vesicle generated through bulk methods is typically 15.8μm/s at 30^oC.[13] However, the values reported in literature varies.[34] DOPC is soluble in ethanol but has been shown to form vesicles in the presence of ethanol mixed aqueous solutions.[28] Phospholipid dispersions in oleic acid were prepared though sonication, 20 minutes at 50^oC. A concentration of 5mg DOPC/ml oleic acid was used as oil phase for all experiments.

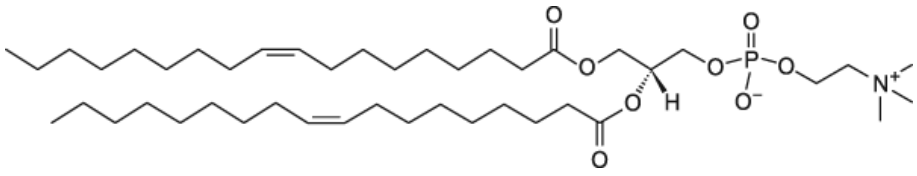

Figure 10: Chemical structure of 1,2-dioleoyl-sn-glycero-3-phosphocholine (DOPC)

DOPC	
Chemical formula	$C_{44}H_{84}NO_8P$
Molecular weight	786.113 g/mol
Transition temperature	-19^oC
Membrane permeability	15.8μm/s

8.2 Membrane dye

To allow fluorescent imaging of the membrane and oil layers the dye 1,1' - dioctadecyl - 3,3,3',3' - tetramethylindocarbocyanine (DiI) was used, see figure 11 for structure. [19] Derivates of DiI have been used to image GUV membranes with phospholipid phase separation. [36]

DiI perchlorate	
Chemical formula	$C_{59}H_{89}ClN_2O_4$
Molecular weight	961.32 g/mol
Abs/Em	549/565nm

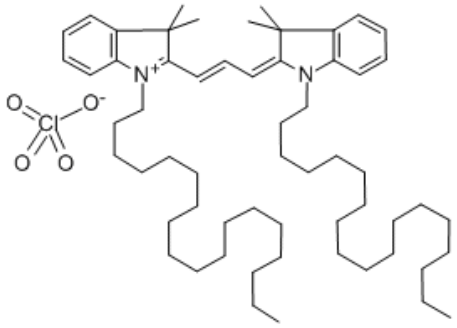

Figure 11: Perchlorate salt of DiI

9 Aqueous phases

9.1 External phase

The external phase is prepared from distilled water, glycerol, ethanol and the surfactant pluronic f68. Glycerol is used to increase the viscosity of the external phase. An increased viscosity is often required for the aqueous phase to be able to exert enough shear on the relatively viscous oil phase. Ethanol serves to extract excess oleic acid from the formed double emulsions. Pluronic f68 is a non-ionic surfactant that stabilizes the formed double emulsions and prevents double emulsion collapse in the initial instances after the generation junction.

Component	Volumetric part
H_2O	1
EtOH	1
Glycerol	1
Pluronic f68 (10% solution)	4

9.2 Internal phase

The internal phase used for vesicle characterization consisted of distilled water with Pluronic f68 added to a concentration of 5%.

To increase the DEP response of vesicles PBS(1x) with 5% Pluronic f68 was used. The conductivity of the internal phase was modified to 14mS/cm by addition of KCl.

10 Experimental setup

The pressure applied to the respective sample reservoirs was set by a computer controlled 4 outlet pressure regulator connected to N_2 gas tubes. Sample reservoir were made from eppendorf tubes and plastic epoxy. Figure 12 shows device setup.

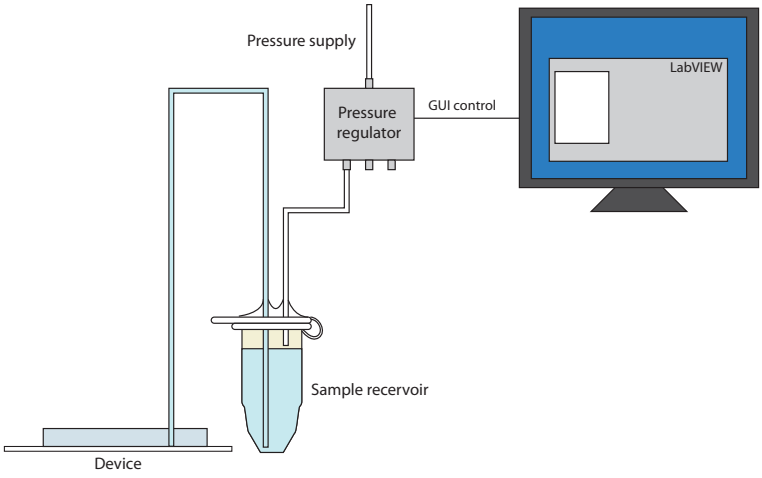

Figure 12: Device setup. Applied pressure is controlled by a computer connected 4 channel pressure regulator. Sample reservoirs made from eppendorf tubes were used.

10.1 Vesicle generation

Figure 13 shows a schematic of the double emulsion generation in an A and B type device. In an A type junction a liquid interface of oil is formed between the internal and external phases as the phases meet in the generation junction. In the case of a B type junction the internal phase is first enveloped by the oil phase in a chamber leading up to the generation junction. In the generation junction the external phase shears off double emulsion from the dispersed phases. The flow rates of the phases is indirectly controlled by setting the pressure applied to sample reservoirs connected to the device inlets.

10.1.1 Solvent extraction

The double emulsions are made into vesicles by extracting the excess oleic acid present in the membrane layer after double emulsion generation. The presence of ethanol renders the oleic acid partially soluble in the external solution and oleic acid is extracted over time. Previous studies have shown that vesicles can be formed from oleic acid containing double emulsions with ethanol soluble and ethanol non-soluble phospholipids.[28][29] To increase the efficiency

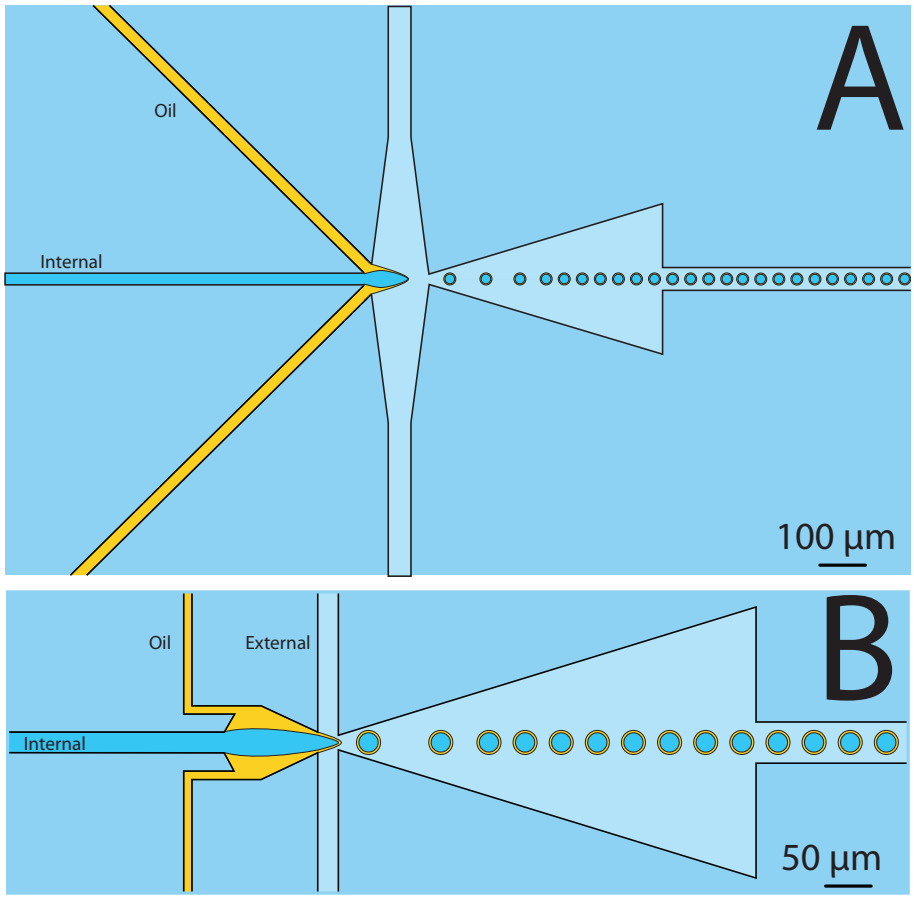

Figure 13: Schematic illustration showing double emulsion generation in junction types A and B.

of extraction iso-propyl alcohol and ethyl-acetate were also used to treat the double emulsions.

10.2 Osmotic pressure shock

Vesicles of different sizes were exposed to an osmotic pressure shock by solubilizing sucrose in the external solution. Sucrose molecules are large relative to solvent molecules and can thus not be transported across the membrane at a rate relevant for the experiment. Sucrose concentration ranged from 0.25 to 2M. Week-old DiI labeled vesicles where injected into a solution containing sucrose and were monitored by time lapse fluorescent imaging. The permeability can be estimated by using equation 3. As water is pumped out from the vesicle the solute concentration inside the vesicle increases and the concentration gradient (Δc) decreases. If

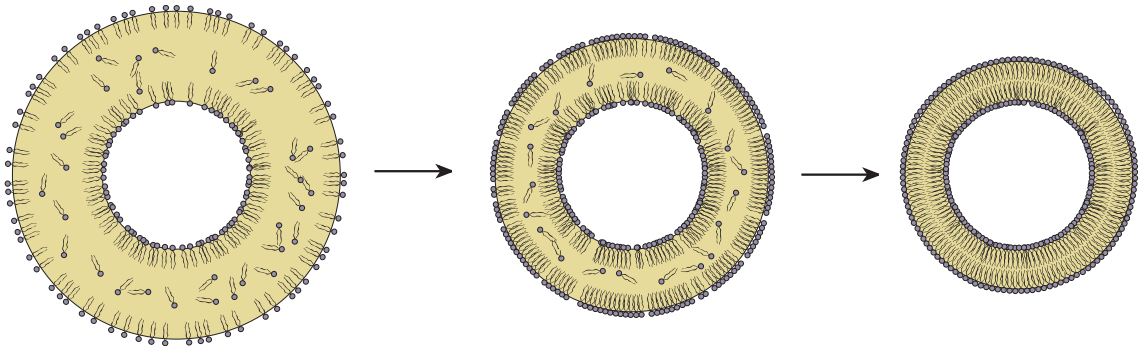

Figure 14: Schematic illustration showing extraction of excess oleic acid resulting in the formation of a lipid bilayer. Relative thickness of membrane layer is exagurated

the vesicles can be followed from t=0 the initial rate, estimated from the first couple of data points, can give a good estimate of the membrane permeability. In this case the change in internal concentration can be neglected. However, if the vesicles cannot be followed from t=0 and the concentration gradient can be assumed to have decreased when the measurements are started another approach is necessary. The process can be modeled by using equation 3 as a starting point, see equations 21 and 22.

$$\dot{r} = -\alpha P \Delta c = -\alpha P(c_{ext} - c_{int}) = -\alpha P(c_{ext} - \frac{3n}{4\pi r^3}), n = c_{int,\infty} V_\infty \tag{21}$$

$$\dot{r} - \frac{3n\alpha P}{4\pi}\frac{1}{r^3} = -\alpha P c_{ext} \tag{22}$$

Equation 22 is a differential equation that describes the response of a vesicle to the osmotic pressure shock. The equation can be solved using numerical methods in e.g. a MATLAB environment. Furthermore, the model can be fitted to an experimental dataset using a non-linear solver and the mean-root-square error (RMSE see equation 23) as the optimization criteria. From the fitted model both the initial vesicle diameter and the membrane permeability can be extracted.

$$RMSE = \sqrt{\frac{\sum (r_{experimental} - r_{model})^2}{n_{datapoints}}} \tag{23}$$

10.3 DEP patterning

The inhomogenous electric fields used for DEP patterning and DEP trapping where created by gold electrodes. Devices were prepared according to above description. 15μm DiI labeled DOPC vesicles with an internal phase containing pluronic, PBS and KCl were used for patterning. Several electrode designs were used, see figure 15. The vesicles were loaded into a

reservoir at the inlet of the DEP device. Flow was generated by applying suction to the outlet of the device. The flow rate was controlled by setting the suction rate of a syringe pump hooked up to the outlet. The electrical signal was generated by a function generator hooked up to an amplifier. A sinusoidal wave was used to actuate the electrodes. Frequencies in the range of 100kHz to 10MHz were used and peak-to-peak voltages ranged from 15 to 80V.

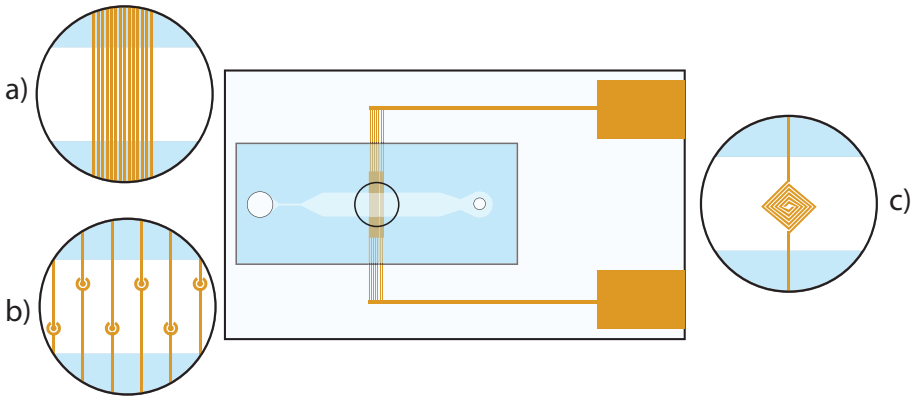

Figure 15: DEP device and electrode patterns used

10.4 Size selective DEP trapping

Two populations of vesicles with different sizes (15 μm and 30μm) were prepared. The populations where mixed and introduced in a device with interdigitated gold electrodes. Flow across the electrodes was induced by applying suction to the outlet by means of a syringe pump. The electric field was generated with a function generator and an amplifier.

Part III
Results and Discussion

11 Vesicle generation

11.1 Device design

In total more than 25 different device designs were tested in order to allow generation of small vesicles at high frequencies.

Initially, devices building on the designs previously developed by *Teh et al.*, utilizing N type junctions, were used to generate vesicles. These devices produces relatively large vesicles (20 to 120 μm) with thick initial oil layers and relatively low generation frequencies. The use of sequentially connected droplet generation junctions limits the flexibility of the vesicle generation. Care must be taken so that the spacing between droplets from the first junction does not allow for any oil droplets to form in the second junction. Aiming to increase the generation rates beyond 1000 Hz and decreasing the vesicle size below 15μm proved to require too much timing and meticulous optimization of the used pressures. However, the sequential method allows for very stable generation and minimal risk of interfacial collapse.

Junction type A was tested to interrogate if generation could be dx using only one junction.

It was observed in N type junctions that if plugs of the internal phase were created by the first junction they were pinched off into multiple vesicles in the second junction. The plugs tended to fill up the channel between the junctions and elongate as they approached the second junction both resulting in thinner initial oil layers. This observation was used to create a hybrid between type N and A, referred to as B. Junction type B allows the internal phase to co-flow with the oil before reaching the junction. The idea was that this would result in a thinner oil phase and make the transition from a rectangular cross section to a circular, conical shape smoother.

11.2 Vesicle size

Vesicles where successfully generated in the size range of 6.5 to 40μm.

As discussed previously, the flow rates are only indirectly controlled when pressure driven flow is used. The Hagen-Poiseuille equation, see equation 5, shows that the pressure drop through a channel is dependent on both the flow rate of the fluid as well as the dimensions of the channel.

In the performed experiments only the pressures supplied to sample reservoirs is known. Since the distances from the device inlets to the junction and the channel widths are different, very little is known about the pressure of each fluid at the generation junction. It is reasonable to assume that the pressures only differ to the extent of the Young-Laplace pressure, see

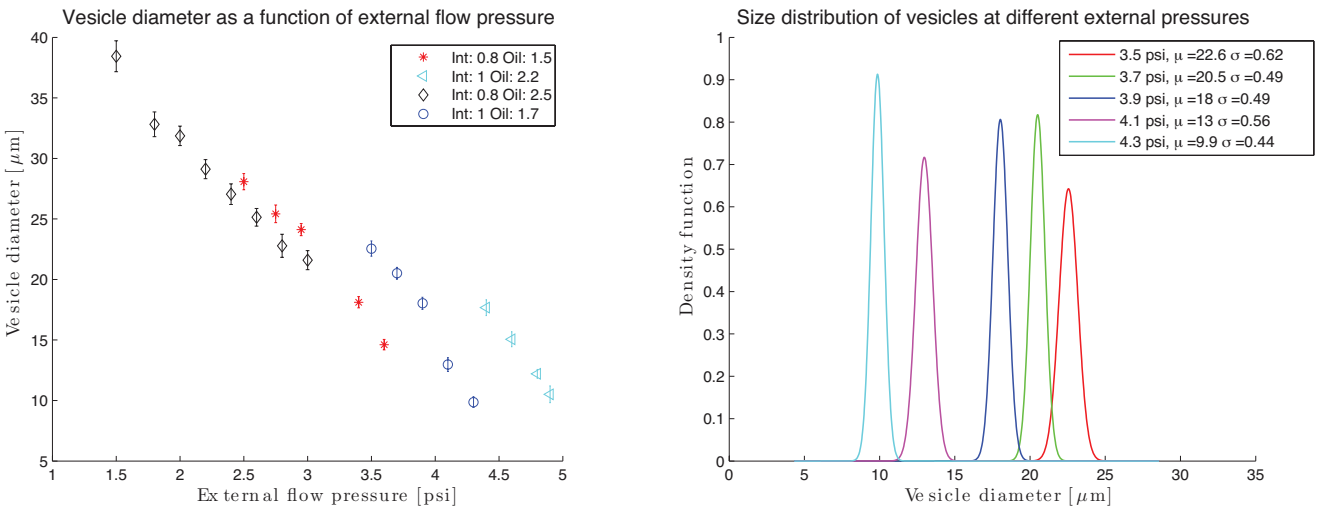

Figure 16: (left) vesicle size as function of external flow pressure and (right) size distribution of vesicle diameters of selected data points. Device B 25 5 17 25 70 10 was used for all experiments

equation 8 and a term causing the fluids to flow relative to each other. Furthermore, a modification of one pressure leads to a change in the flow rate of all phases, not just the modified phase. This considerably increases the complexity of data analysis. If a finite volumetric flow can be assigned to each phase, all experimental data can be interpreted in terms of relative flow rates. For pressure driven flow this is not the case. Experimental data series where one pressure is incrementally modified can readily be interpreted, but comparison between data where more than one pressure is modified gives limited information.

Vesicle size as function of external flow pressure is displayed in figure 16. No pressure setting was able to sustain stable vesicle generation in the entire range of examined vesicle diameters. Several data sets with modified relative pressures were therefore captured. The data sets also give information on the effect of changing one or more pressures. Within every dataset the vesicle size decreases monotonically as the external pressure is increased. Vesicle size appears to decrease linearly within each data series. An increase in oil pressure relative to the pressure on the internal phase appears to shift the data series towards higher external pressures, indicating that a higher external pressure is needed to shear off a droplet. It is reasonable to assume that an increase in the combined pressure of the internal and oil phases will lead to an increase in the external pressure required to shear off a droplet, which thus is supported by the experimental findings. Furthermore, the vesicle size was observed to be highly dependent on the pressure of the internal phase, a small change drastically affected the size of the generated vesicles and often forced the generation into an unstable regime.

From the captured images of double emulsion generation in figure 17 three distinct modes

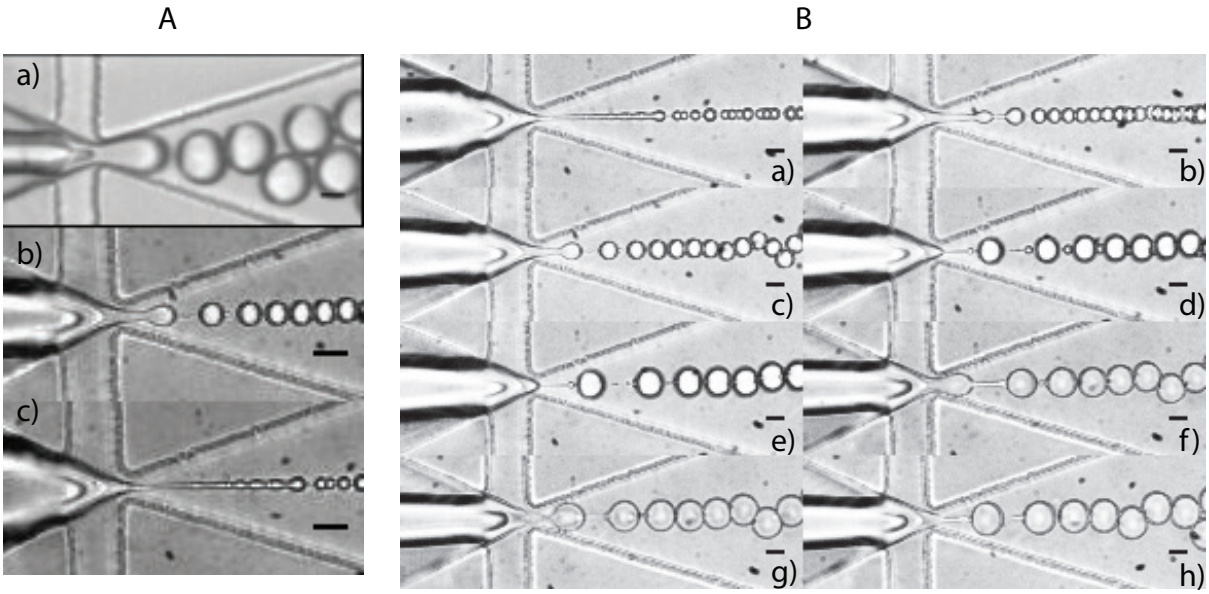

Figure 17: (A) Figures displaying vesicle generation regimes. Dripping regime (a), intermediate regime (b) and jetting regime (c). Scale bar 20μm. (B) Table of vesicle sizes. Scale bar 15μm. Vesicle sizes a) 6.3μm b) 9.3μm c) 12.4μm d) 18.1μm e) 20.6μm f) 21.4μm g) 22.5μm h) 23.4μm

of double emulsion generation can be identified. These regimes are very similar to the regimes discussed in a previous section. At low external phase pressure the entire liquid interface is retracting as a result of double emulsion break off. Break off occurs beyond the junction orifice. This regime displays all characteristics of the dripping regime observed for single emulsion droplet generation in flow focusing devices. At intermediate pressures the liquid interface appears more fixed to the orifice of the generation junction and only the very tip of the interface is retracting, the generated sizes are smaller and the generation frequency significantly higher. At high pressures the generation moves into the jetting regime where the interface is completely fixed and the break off occurs beyond the actual generation junction. The double emulsions produced in this region are very small but tend to coalesce uncontrollably. In summary the characteristics of the generation closely follows the rationales of droplet generation in standard flow focusing devices.

From images of the generation process it is clear that the liquid interface goes from a rectangular shape defined by the channel dimensions to a conical shape in three dimensions lacking contact with the channels walls in the generation junction. It is therefore evident that this method allows efficient double emulsion generation without special equipment supporting the creation of a symmetric interface, such as that used by Shum *et al.*.

11.3 Generation frequency

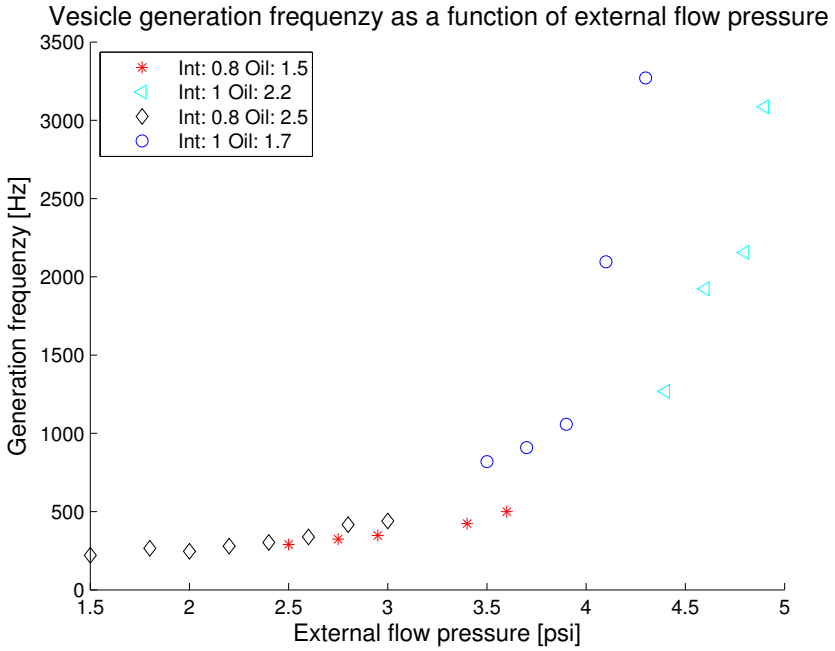

Figure 18: Vesicle generation frequency as function of external flow pressure. Device B 25 5 17 25 70 10 was used for all experiments

The vesicle generation frequency as a function of external pressure can be seen in figure 18. The results show a drastic increase in generation frequency at high pressures. This can be explained by considering the relationship between vesicle diameter and generation frequency, see equation 24 where f is the generation frequency, Q_d is the flow rate of the dispersed phases (internal + oil) and V_v is the volume of one vesicle.

$$f = \frac{Q_d}{V_v} = \frac{6Q_d}{\pi d^3} \tag{24}$$

As previously discussed the diameter decreases linearly within each data set. If the volumetric flow rate of the dispersed phases can be assumed to be constant, equation 24 gives an inverse cubic relationship between the generation frequency and the vesicle diameter ($f \sim \frac{1}{d^3}$). By assuming that the flow rate of the dispersed phases is proportional to the ratio between the sum of the pressures of the dispersed phase and the pressure of the external phase ($Q_d \sim \frac{p_{int}+p_{oil}}{p_{ext}}$) a normalized frequency can be calculated using equation 24, see figure 19. The results show that the increase in frequency follows the general trend of the calculated frequency but that the

increase is less drastic. The discrepancy could possibly be explained by considering that the flow of the dispersed phases in fact is not constant over the range of external phase pressures. The flow of the dispersed phase will likely decrease somewhat due to the competition with the pressure of the external phase.

The drastic increase in generation frequency can also be explained by considering that the generation moves towards the jetting regime at higher external phase pressures. In this regime the Rayleigh-Plateu timescale will dominate over the time scale of the volumetric flow, resulting in increased occurrence of droplet break off. Utada *et al.* described a initial decrease in double emulsion diameter as the jetting regime is approached, followed by a drastic increase in diameter and decrease in generation frequency when passing a certain threshold flow rate. In this study the vesicle diameter decreases as the pressures are increased and the jetting regime is approached but no sudden increase is observed.

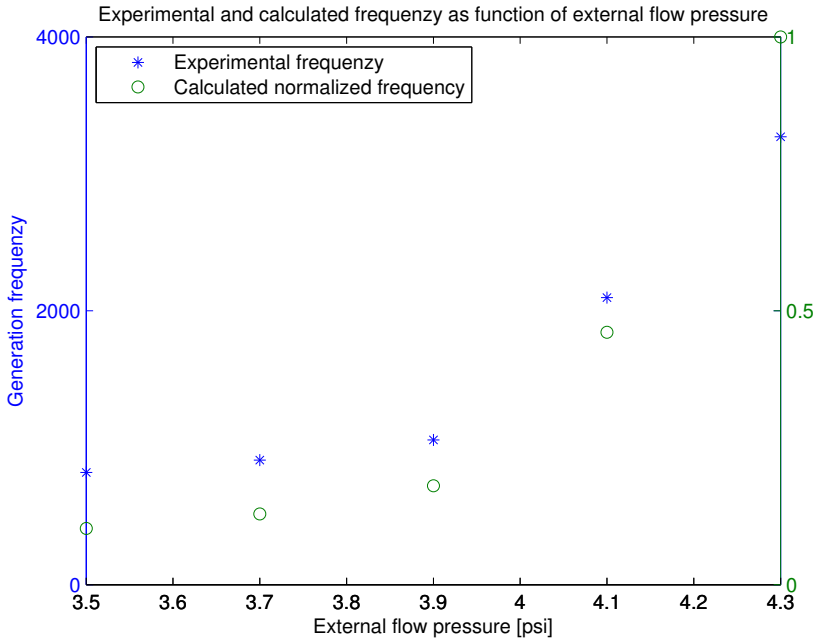

Figure 19: Vesicle generation rate as function of external flow pressure. Experimental and calculated frequency

In order to take this reasoning further it would be interesting to try and estimate the capillary number from the experimental data and see if it matches the rationale of transition from dripping to jetting regime. Equation 12 relates the dynamic parameter of the generation to the capillary number. Assuming that the flow of the dispersed phases can be estimated

from the mean diameter and the frequency Q_{disp} can be calculated. The radius of the jet can be estimated from the droplet diameter and the viscosity of the external phase can be calculated considering the ration of solvent used. Although the surface tension of pure solvents generally are tabulated in literature, it is hard to estimate the interfacial tension between two liquid phases and further more take into account the effect of surfactants. At a surfactant concentration of about 5% of Span (polysorbate) in mineral oil the interfacial tension has been reported to be 0.01N/m[17]. In lack of a value that more closely captures the system at hand this will serve as an estimation. The result of the calculation are shown in figure 20. Interestingly this rough estimation accurately captures the transition from dripping to jetting regime. It appears that the data points from experiments at higher external pressures stretch beyond the $Ca \approx 1$ threshold indicative of the transition. It is therefore likely that the generation moves towards a jetting regime as the external pressure is increased.

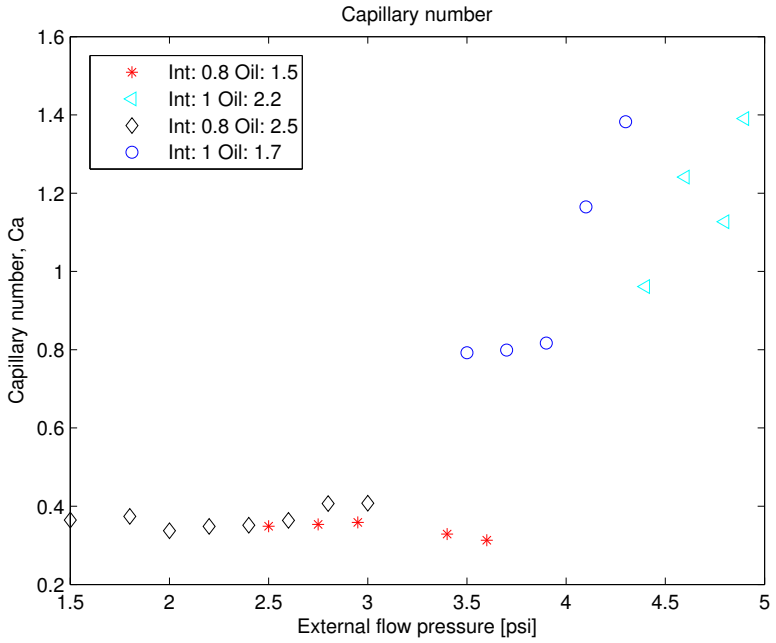

Figure 20: Capillary number as function of external flow pressure. Estimated from experimental data and assumptions on interfacial tension

11.4 Device comparison

Up to this point the device B 25 6 17 25 70 10 was used for all experiments. To illustrate the effect of geometry on the vesicle generation a device with thinner channels and orifice (B 10

10 6 17 10 30 10) was tested. As can be seen in figure 21 the slope of the vesicle diameter as a function of external phase pressure in device B 10 10 6 17 10 30 10 is considerably lower than that of device B 25 6 17 25 70 10 at equivalent pressures. Furthermore, this results in that an external phase pressure exceeding 5psi (the upper limit of the experimental setup) is required to generate vesicles smaller than 10μm. Both these effects are likely due to an increase in channel resistance due to the decreased channel dimensions, according to Hagen-Poiseuille's law.

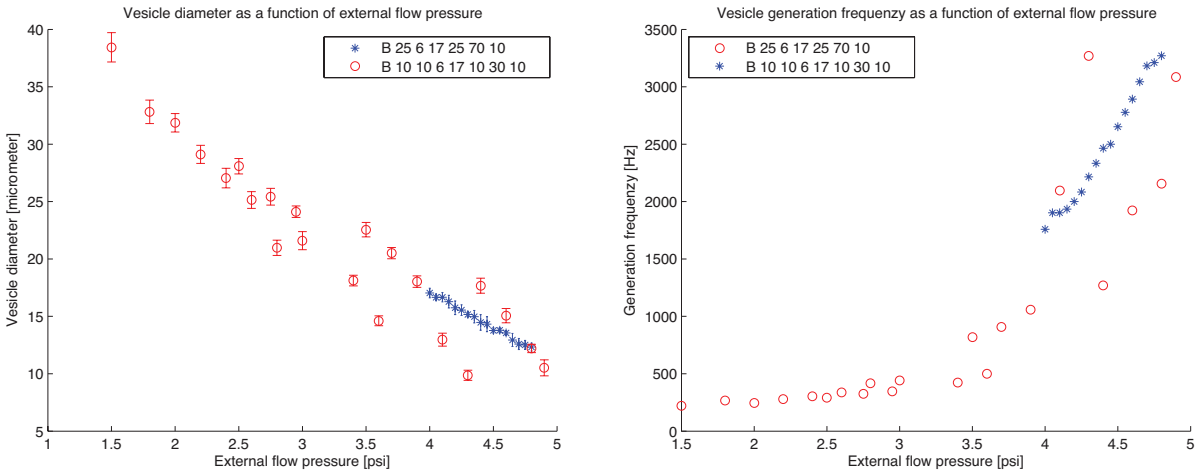

Figure 21: (left) vesicle size and (right) generation frequency as function of external flow pressure comparing two device designs

12 Vesicle characterization

It was observed that smaller vesicles ($d < 15\mu$m) tended to have a relatively thicker residual oil layer after extended extraction in standard external phase (14% ethanol) than larger vesicles. Generated vesicles where transferred to solutions containing isopropanol (IPA), ethyl acetate (EtAc) or increased concentration of ethanol (EtOH) in order to attempt to extract more of the oleic acid, see table 1.

The results of these more aggressive attempts to remove excess oleic acid are shown in figure 22. It is evident that an increase in ethanol concentration thins out the membrane layer. At 40% (S4) the membrane layer appears thin and well distinguished. The effect is more drastic in the case of IPA and EtAc. In sample 7,10 and 11 the membranes are very well distinguished. Although the fluorescent images indicate a considerable thinning out of the membrane the images cannot be used to directly measure the thickness of the membrane. When

Table 1: Prepared extraction solutions

Sample #	Ethanol [%]	Isopropanol [%]	Ethyl-acetate [%]
1	14	0	0
2	20	0	0
3	30	0	0
4	40	0	0
5	14	5	0
6	14	10	0
7	14	20	0
8	14	0	1
9	14	0	5
10	14	0	10
11	14	5	5

the fluorophores relax and emit radiation the signal broadens considerably due to diffraction. Furthermore, no feature smaller than the wavelength of the light can be resolved. Another interesting phenomena occurred in sample 7 and 11. If the bright field microscope focal plane was put on the waist of the vesicle the contrast at which the vesicle was resolved decreased drastically, while the vesicle remained well distinguishable when observed slightly off focus. This is a clear indication the the vesicle membrane layers have thinned out considerably and that the membrane thickness is smaller than the wavelength of the light used to observe them.

12.1 Osmotic pressure shock

Double emulsions readily shrunk as a result of an imposed osmotic pressure shock, see figure 23. Both double emulsions in standard external phase and double emulsion treated with 20% IPA were subjected to osmotic pressure shock. Figure 24a indicates that the initial slope of a vesicle treated with IPA is approximately the same as the slope of an untreated double emulsion subjected to an 8 times stronger concentration gradient. This is another indication that there is a significant difference in membrane layer thickness between the two.

More detailed determination of the permeability was conducted on vesicles treated with 20% IPA. Using MATLAB, the mathematical model for the osmotic shock (equation 22) can be fitted to the experimental data, see figure 24. Optimization of the fit gives a permeability of approximately 10 μm/s. The permeability is thus just outside range of what is expected of a vesicle. Permeabilities ranging from 45μm/s [34] to 15.8μm/s [13] have been reported for DOPC. The calculated value is also in good agreement with reported experimental values for vesicles generated by other microfluidic methods (13-15.7μm/s).[18]. It is likely that some oleic acid remains in the membrane layer even after extensive extraction. This would make

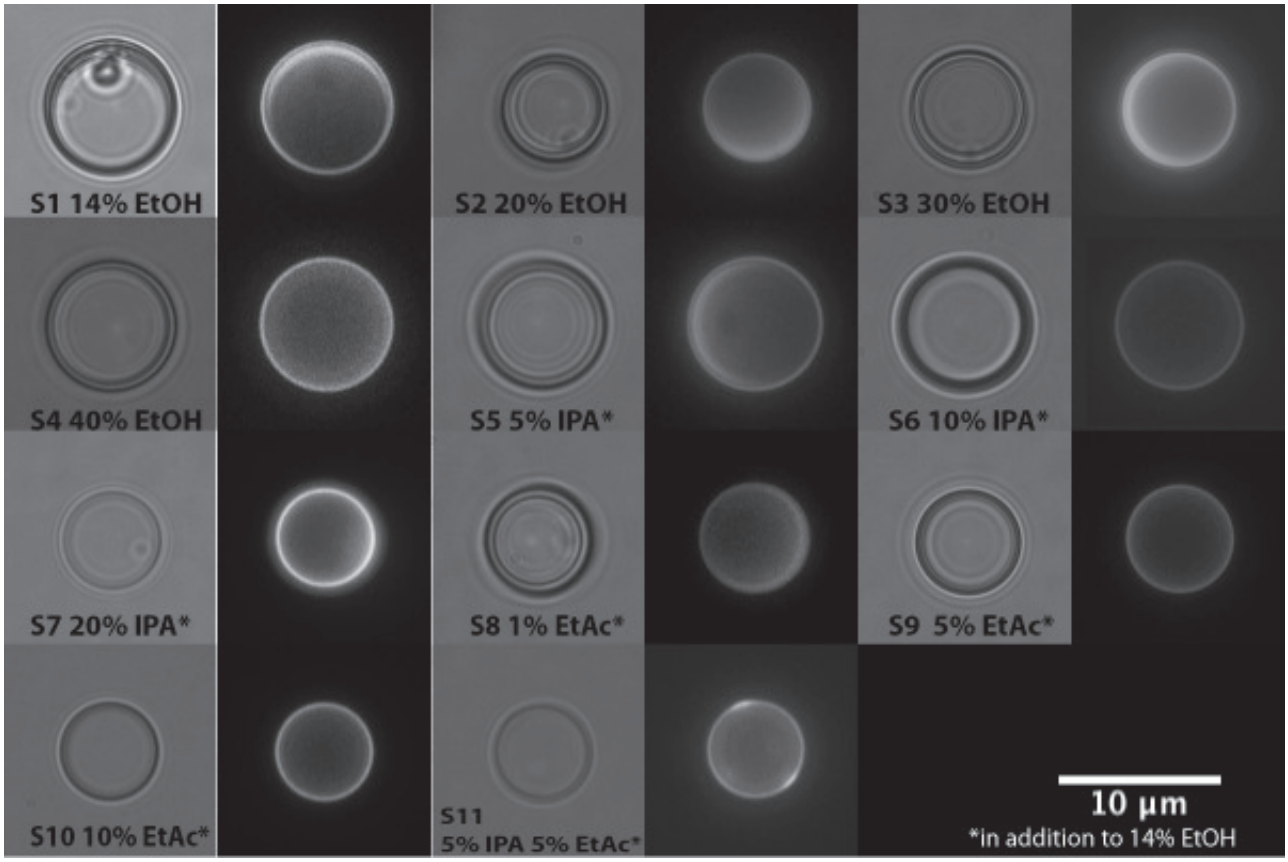

Figure 22: Double emulsion before and after ethanol, IPA and/or ethyl acetate treatment. Pairwise bright field and fluorescent imaging of generated double emulsions. Membrane layer labeled with DiI.

some regions of the membranes thicker and decrease the permeability. Since the calculated value is very close to the range expected of vesicles it is likely that the vesicles produced have at least partial lipid bilayers. Several experimental factors may also influence the measured permeability towards lower values. There is great deal of uncertainty in the actual sucrose concentration immediately outside the vesicle. No mixing is induced when the vesicles are introduced in the osmotic shock medium and thus the concentration is built up as sucrose diffuses from the bulk solution. Furthermore, the sucrose and the glycerol used gives the external medium a high viscosity, resulting in slow diffusion rates. All these factors contribute to make the measured permeability lower than the actual permeability of the membrane.

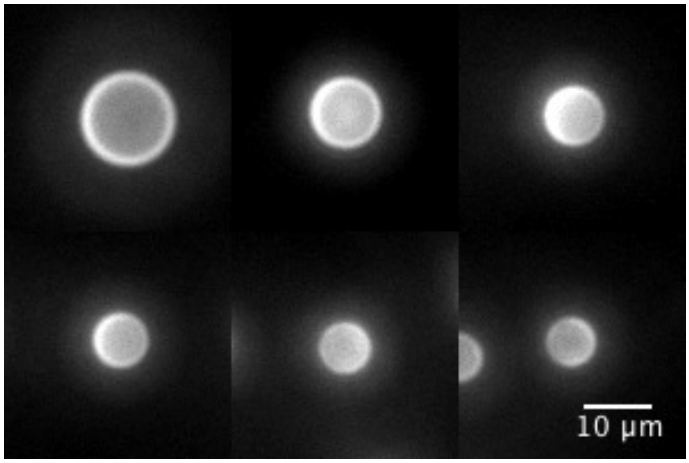

Figure 23: Double emulsion response to osmotic shock. Sucrose concentration 2M. Frame rate 1 frame per minute

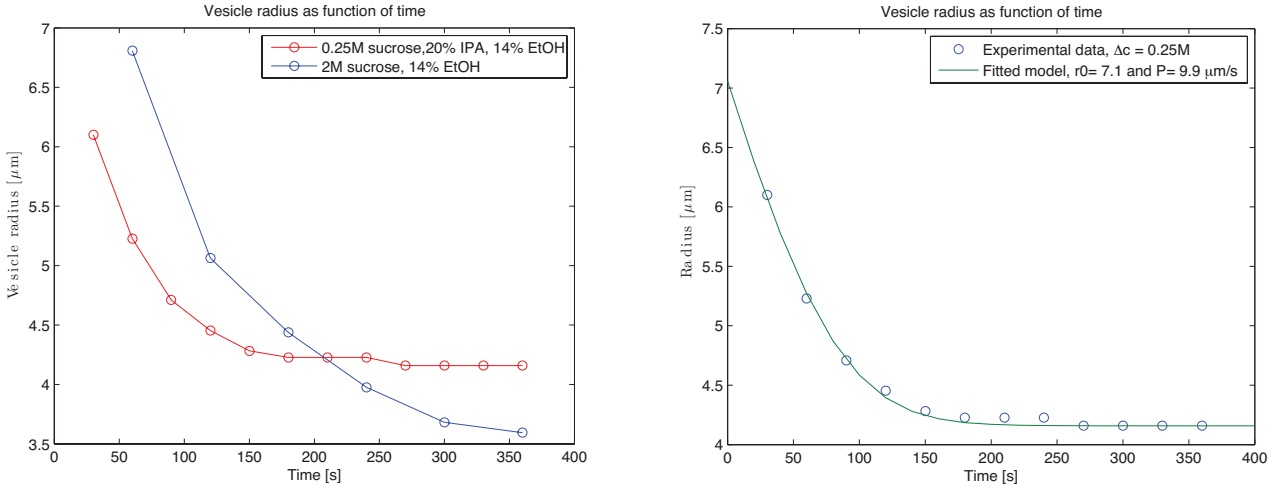

Figure 24: Double emulsion response to osmotic shock. Radius as function of time. (a) untreated and IPA treated double emulsions (b) IPA treated double emulsion with fitted mathematical model

13 DEP

13.1 Particle modeling

Equation 18 can be used to estimate the f_{CM} factor for the double emulsions generated and help determine an appropriate frequency range for the electric field. The shell model also

allows for modeling of the effect of vesicle size and membrane thickness.

Model variables		
Permittivity of vacuum	ϵ_0	$8.85 \cdot 10^{-12}$ F/m
Relative permittivity (internal)	ϵ_{int}	80.1
Conductivity (internal)	σ_{int}	$8.2 \cdot 10^{-1}$ S/m
Relative permittivity (membrane)	ϵ_m	10
Conductivity (membrane)	σ_m	$8.2 \cdot 10^{-9}$ S/m
Membrane thickness	l	10nm
Relative permittivity (external)	ϵ_{ext}	80.1
Conductivity (external)	σ_{ext}	$5 \cdot 10^{-5}$ S/m

The Clausius-Mosotti factor was calculated using the shell model for a variety of vesicle diameters, see figure 25a. The results show a strong positive DEP response for vesicles larger than 1μm at field frequencies between 10kHz and 10MHz. Apart from the fact that a difference in size gives a change in the DEP force on a particle according to equation 17, f_{CM} will also affect the DEP response.

The membrane acts as an insulating layer outside the highly conductive aqueous core. Since the generation method relies on the extraction of the oil layer, resulting in a gradual degrease in the layer thickness it is of interest to examine the effect of layer thickness on the DEP response. Figure 25b shows f_{CM} for a 10μm vesicle with a oil layer of varying thickness. The results show that increasing oil layer thickness leads to a weaker positive DEP response and a stronger response to negative DEP. From experimental data it is estimated that the double emulsions have 500nm oil layers after extraction in 14% ethanol.

In order to model the experimental settings where 30μm vesicles were selectively trapped in the presence of 15μm vesicles f_{CM} was calculated, see 25c. The results show that f_{CM} acts in favor of selective trapping by increasing the DEP response of larger vesicles relative to smaller. The increased response due to the f_{CM} factor combined with the inverse relationship between the trapping field gradient and the double emulsion radius should result in larger vesicles being trapped at significantly lower voltages than smaller ($\nabla|E_{rms}|^2_{trap} \sim \frac{1}{r^2}$).

13.2 DEP patterning

In many instances it would be very useful to be able to control the two dimensional organization of vesicles that are intended for assaying or analysis. Furthermore, it might be beneficial for down stream processing and vesicle loading if the arrangement of vesicles could be controlled. Vesicle patterning through the use of DEP is one possible way to achieve this. By designing electrodes so that regions of high electric filed strength are created in a foreseeable manner, vesicle patterning can be achieved. As described in a previous section a number of different electrode designs were created. For the purpose of DEP pattering 15μm vesicles were used. The setup allows for three controlling parameters set by the operator; the applied voltage and frequency as well as the imposed flow rate.The voltage and the flow rate have directly opposing effects. An increased flow rates makes the vesicles harder to trap due to the increase in Stokes

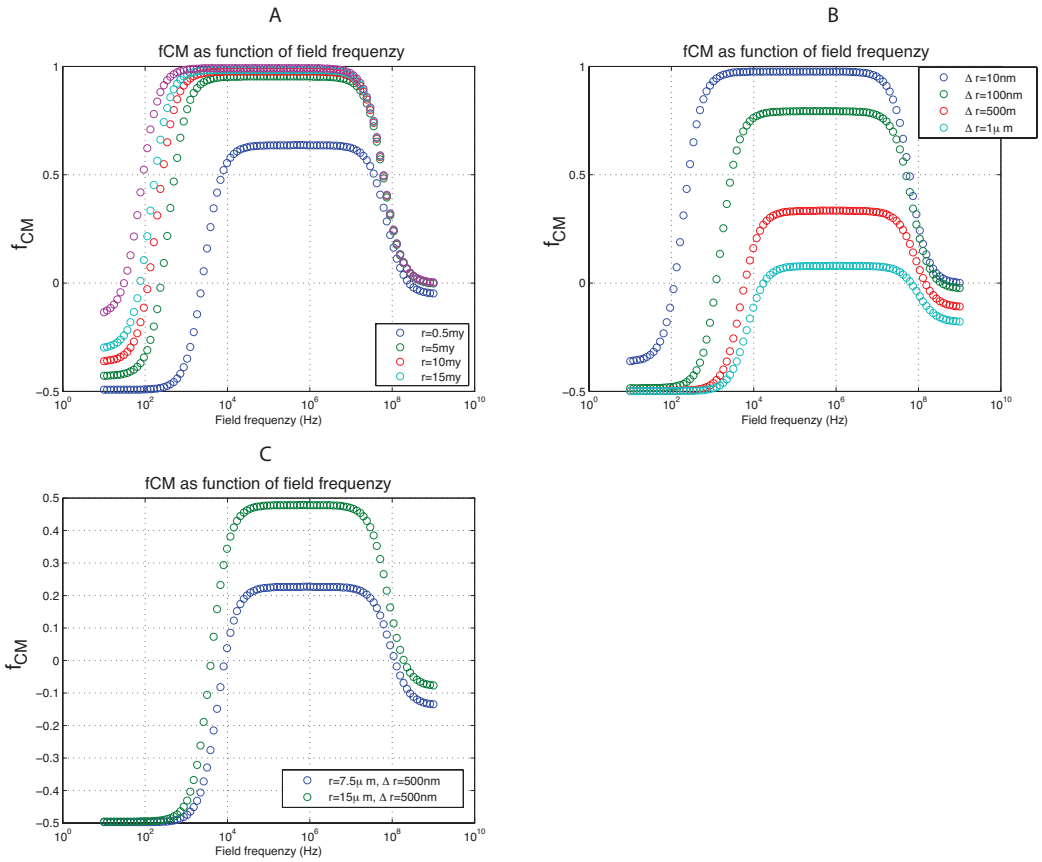

Figure 25: f_{CM} as function of electric field frequency and (A) double emulsion size and (B) membrane thickness. (C) displays experimental setup.

drag on the particle. An increase in applied voltage increases the potential difference between the electrodes. This results in a stronger electric field gradient, a stronger DEP force and a higher probability for vesicle trapping, see equation 20. 15μm vesicles trapped at almost complete efficiency at a flow rate of 0.3μl/min, an applied electric voltage of 60V_{pp} and a field frequency of 750kHz. The resulting patterns can be seen in figure 26. The interdigitated electrodes gave rise to a barred pattern with well-defined vesicle bars. The first couple of bars generally displayed a lower trapping efficiency (seen as a lower fluorescent intensity) due to the characteristic time it takes for the vesicles to move from the bulk of the solution to the surface of the electrodes and be retarded enough by the DEF force to finally be trapped. The spiral electrode configuration displayed both transient and terminal patterning of vesicles. Vesicles flowing across the electrodes with the electric field on continued to move along the the tangent of the electrodes until they where trapped in the terminal pattern.

The vesicles gathered in the terminal pattern in high densities and could be released as plugs. Dotted electrodes gave rise to well defined patterns where vesicles only trapped in the intended spots.

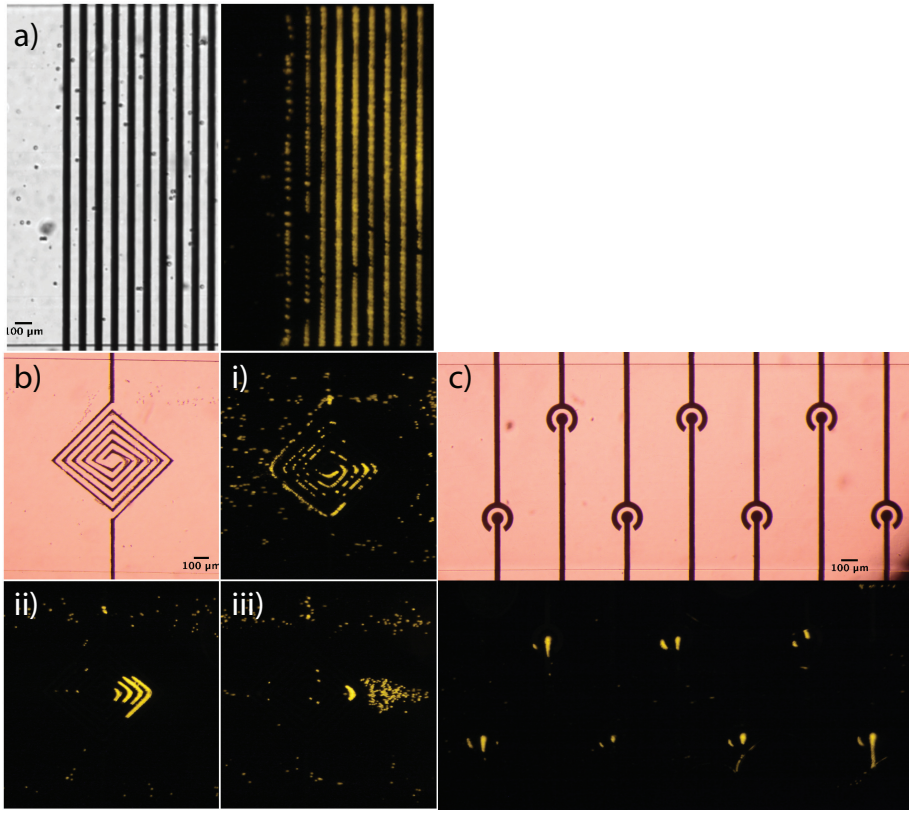

Figure 26: Patterns generated through DEP. a) interdigitated electrodes (50μm spacing), b) spiral pattern and c) dotted electrodes. b,i) transient pattern, b,ii) terminal pattern and b,iii) release of collected vesicles. Flow from left to right. Vesicle trapped at 0.3μl/min, 750kHz and 60V_{pp}

It was observed that vesicles with diameters comparable to the distance between to neighboring electrode tended to burst at higher flow rates and voltages. This is possibly due to the fact that a vesicle of this size will be pulled towards two neighboring regions of high electric field strength and thus be pulled apart. Alternatively, the increased viscous drag at higher flow rates combined with a stronger DEP force might deform the vesicle to a point where it collapses. Vesicles 15μm and smaller were observed to withstand a vide range of flow rates and voltages.

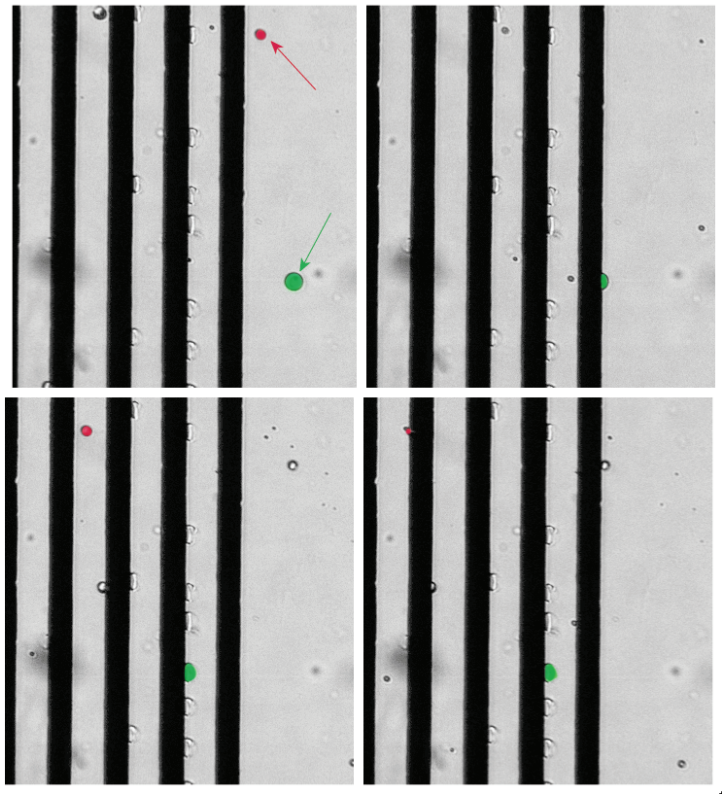

Figure 27: Selective trapping of large vesicles. Initial position of 30μm and 15μm vesicle indicated with green and red arrow respectively. Flow form right to left. Flow rate was set to 0.2μl/min, field frequency to 750kHz and applied voltage of $20V_{pp}$

13.3 Selective DEP trapping

As discussed previously, DEP presents an attractive way to allow complex manipulation of vesicles. One such use could be to selectively trap a subset of a mixed population of vesicles in order to isolate the subset or eliminate it from the mixed population. DEP trapping is dependent to both size and chemistry of the affected particle. However, the size dependence is much stronger in most cases, see equation 20. Therefore experiments attempting to trap only the larger vesicles in a bidispersed population containing 30μm and 15μm vesicles were conducted. At a voltage of 20V, a frequency of 750kHz and a flow rate of 0.2μl/min only the 30μm subpopulation was observed to trap, see figure 27. It is also very important that the vesicles can be released without compromising their integrity and ability to be resuspended in the medium. Experiments showed that after trapping, the vesicles could readily be released and resuspended into the medium, see figure 28.

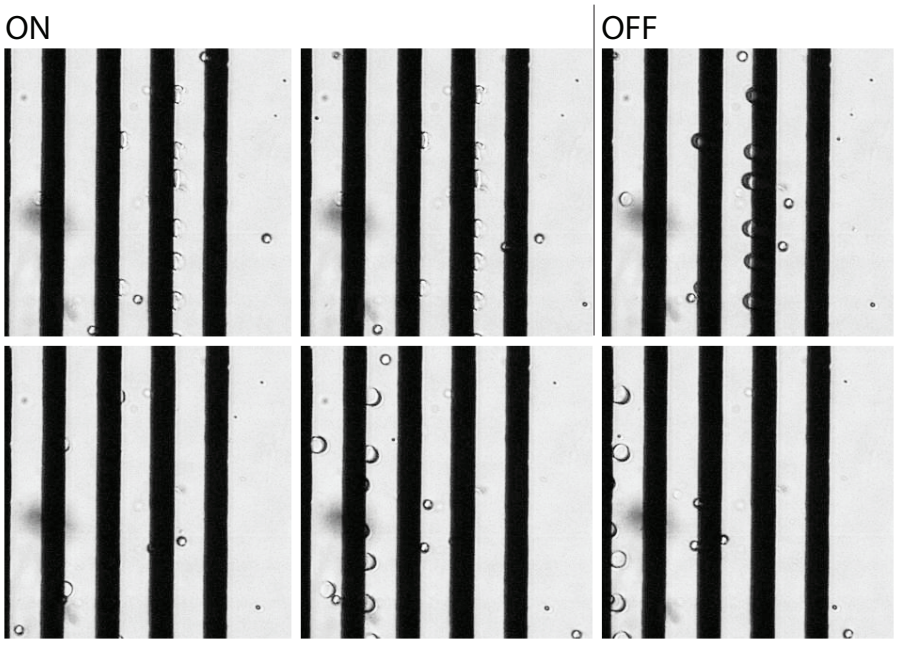

Figure 28: Release of selectively trapped large vesicles. 30μm vesicle trapped when field is ON and resuspended when field is turned OFF. Flow form right to left. Flow rate was set to 0.2μl/min, field frequency to 750kHz and applied voltage of $20V_{pp}$

Part IV
Conclusion

GUVs offer compelling advantages as model systems for biology, biosensors and biomicroreactors compared to many other systems. However, in order to allow GUVs to reach their full potential, robust, efficient and flexible generation methods are crucial.

The method described in this report allows for generation of vesicles in a wide size range (6.5-45μm) at high generation frequencies (300-3500Hz). Vesicles are created from double emulsion templates generated in a single-step flow focusing device.

Extraction of the excess solvent from the generated double emulsions is shown to transform them into vesicle like assemblies with characteristics similar to vesicles generated though bulk and other microfluidic methods. The most compelling benefit of the method is thus that it allows high throughput generation of cell-sized vesicles.

The proposed method addresses many of the issues encountered with other microfluidic methods. The membrane interface in the generation junction is continuously replenished allowing for truly continuous double emulsion generation. The generation is stable and uniform over time, unlike some reports of other methods[18]. The external and internal phases are addressed separately and can readily be tailored to suit the intended application.

Some proposed methods require assembly of miniature systems made up of small independent parts such as glass capillaries and modified ink jet dispensers. These devices require careful assembly and are only suitable for serial manufacture. The method described in this report relies solely on standard photo and soft lithography techniques making batch fabrication both possible and straightforward. Results show that the semi 3D environment created in these devices fully supports the efficient generation of double emulsions without the need of true 3D or cylindrical components.

In order to efficiently perform GUV based assays and create complex GUV based model systems, sophisticated tools for vesicle manipulation are required. In this report DEP is proposed as one such tool. DEP allows for transient, size and composition dependent trapping and patterning. Subpopulations of vesicles can be targeted in a larger population displaying a range of vesicle sizes. DEP can thus be used as a tool for sample enrichment and isolation by either trapping the desired subpopulation or the unwanted size fractions. By continuing the work to investigate the relationship between vesicle composition and chemistry with its characteristic DEP response more specific and selective DEP-GUV systems will emerge, allowing more complexity in system design. The need for a flexible generation method is thus even more pronounced. The DEP work described in this report serves as an initial indication of the potential and wide applicability of DEP-GUV systems.

In the immediate future more in-depth membrane characterization is necessary to prove that the membranes are true bilayers. Definitive bilayer determination is done through sample freezing and SEM imaging. A more low-tech alternative would be to observe the integration

of α-hemolysin into the lipid bilayer. α-hemolysin integration is considered a strong indication that true bilayers are present.

There is an endless variety of possible electrode designs and combinations of designs. GUV patterning could be improved by optimizing the electrode design. For example a more well defined vesicle plug could likely be released from a different set of electrodes. An array of interdigitated electrode patterns with different applied voltage could be used to trap several size fraction in the same device, allowing assaying of different things in different parts of the device. GUV patterns were generally very well defined and only resulted in vesicle trapping in the intended regions. Dotted electrodes allows for several small and well defied sets of vesicles to be collected from a larger population. The vesicles could be easily be loaded into downstream processing units due to their high packing density and well defined pattern. Since the GUV size is very closely controlled by the generation method, the size itself could serve as a label free marker for mixed populations of vesicles with different assays. DEP should also be explored as a method to selective trap a subpopulation bases on chemistry or composition. DEP theory supports such selectivity and it would add another dimension to the range of manipulations and trapping criteria that could be constructed.

References

[1] A Castellanos, A Ramos, and A Gonzalez. Electrohydrodynamics and dielectrophoresis in microsystems: scaling laws. *Journal of Physics D: ...*, 2003.

[2] Barnabé Chaize, Michel Nguyen, Tristan Ruysschaert, Véronique le Berre, Emmanuelle Trévisiol, Anne-Marie Caminade, Jean Pierre Majoral, Geneviève Pratviel, Bernard Meunier, Mathias Winterhalter, and Didier Fournier. Microstructured Liposome Array. *Bioconjugate chemistry*, 17(1):245–247, January 2006.

[3] Vittorio Cristini and Yung-Chieh Tan. Theory and numerical simulation of droplet dynamics in complex flows a review. *Lab on a Chip*, 4(4):257, 2004.

[4] Salil P Desai, Michael D Vahey, and Joel Voldman. Electrically Addressable Vesicles: Tools for Dielectrophoresis Metrology. *Langmuir*, 25(6):3867–3875, March 2009.

[5] Victoria E Froude and Yingxi Zhu. Dielectrophoresis of Functionalized Lipid Unilamellar Vesicles (Liposomes) with Contrasting Surface Constructs. *The Journal of Physical Chemistry B*, 113(6):1552–1558, February 2009.

[6] A Günther and KF Jensen. Multiphase microfluidics: from flow characteristics to chemical and materials synthesis. *Lab on a Chip*, 6(12):1487–1503, 2006.

[7] MJ Hope, MB Bally, LD Mayer, and AS Janoff. Generation of multilamellar and unilamellar phospholipid vesicles. *Chemistry and physics of ...*, 1986.

[8] Nikhil D Kalyankar, Manoj K Sharma, Shyam V Vaidya, David Calhoun, Charles Maldarelli, Alexander Couzis, and Lane Gilchrist. Arraying of Intact Liposomes into Chemically Functionalized Microwells. *Langmuir*, 22(12):5403–5411, June 2006.

[9] Brian J Kirby. *Micro- and Nanoscale Fluid Mechanics*. Transport in Microfluidic Devices. Cambridge Univ Pr, July 2010.

[10] J Korlach, C Reichle, T Müller, T Schnelle, and W W Webb. Trapping, Deformation, and Rotation of Giant Unilamellar Vesicles in Octode Dielectrophoretic Field Cages. *Biophysical Journal*, 89(1):554–562, July 2005.

[11] Mikhail Kozlov, Mamle Quarmyne, Wei Chen, and Thomas J McCarthy. Adsorption of Poly(vinyl alcohol) onto Hydrophobic Substrates. A General Approach for Hydrophilizing and Chemically Activating Surfaces. *Macromolecules*, 36(16):6054–6059, August 2003.

[12] J Liu, B Cai, J Zhu, G Ding, X Zhao, C Yang, and D Chen. Process research of high aspect ratio microstructure using SU-8 resist. *Microsystem Technologies*, 10(4):265–268, May 2004.

[13] J C Mathai, S Tristram-Nagle, J F Nagle, and M L Zeidel. Structural Determinants of Water Permeability through the Lipid Membrane. *The Journal of General Physiology*, 131(1):69–76, December 2007.

[14] NT Nguyen. Fundamentals and applications of microfluidics, 2002.

[15] V Noireaux, R Bar-Ziv, J Godefroy, H Salman, and A Libchaber. Toward an artificial cell based on gene expression in vesicles. *Physical biology*, 2:P1, 2005.

[16] V Noireaux and A Libchaber. A vesicle bioreactor as a step toward an artificial cell assembly. *Proceedings of the National Academy of Sciences of the United States of America*, 101(51):17669, 2004.

[17] FO Opawale. Influence of Interfacial Properties of Lipophilic Surfactants on Water-in-Oil Emulsion Stability* 1. *Journal of colloid and interface science*, 1998.

[18] S Ota and S Yoshizawa. Microfluidic Formation of Monodisperse, CellSized, and Unilamellar Vesicles. *... Chemie International Edition*, January 2009.

[19] R E Pitas, T L Innerarity, J N Weinstein, and R W Mahley. Acetoacetylated lipoproteins used to distinguish fibroblasts from macrophages in vitro by fluorescence microscopy. *Arteriosclerosis (Dallas, Tex.)*, 1(3):177–185, April 1981.

[20] J P Reeves and R M Dowben. Formation and properties of thin-walled phospholipid vesicles. *Journal of cellular physiology*, 73(1):49–60, February 1969.

[21] Hirohide Saito, Yusho Kato, Maël Le Berre, Ayako Yamada, Tan Inoue, Kenichi Yosikawa, and Damien Baigl. Time-Resolved Tracking of a Minimum Gene Expression System Reconstituted in Giant Liposomes. *ChemBioChem*, 10(10):1640–1643, July 2009.

[22] Minseok Seo, Zhihong Nie, Shengqing Xu, Michelle Mok, Patrick C Lewis, Robert Graham, and Eugenia Kumacheva. Continuous Microfluidic Reactors for Polymer Particles. *Langmuir*, 21(25):11614–11622, December 2005.

[23] Ho Cheung Shum, Daeyeon Lee, Insun Yoon, Tom Kodger, and David A Weitz. Double Emulsion Templated Monodisperse Phospholipid Vesicles. *Langmuir*, 24(15):7651–7653, August 2008.

[24] JC Stachowiak and DL Richmond. Unilamellar vesicle formation and encapsulation by microfluidic jetting. In *Proceedings of the ...*, 2008.

[25] NG Stoicheva. ScienceDirect - Biochimica et Biophysica Acta (BBA) - Biomembranes : Dielectrophoresis of cell-size liposomes. *Biochimica et Biophysica Acta (BBA)- ...*, 1994.

[26] Pia Streicher, Pierre Nassoy, Michael Bärmann, Aurélien Dif, Valérie Marchi-Artzner, Francoise Brochard-Wyart, Joachim Spatz, and Patricia Bassereau. Integrin reconstituted in GUVs: A biomimetic system to study initial steps of cell spreading. *BBA - Biomembranes*, 1788(10):2291–2300, October 2009.

[27] Kingo Takiguchi, Ayako Yamada, Makiko Negishi, Yohko Tanaka-Takiguchi, and Kenichi Yoshikawa. Entrapping Desired Amounts of Actin Filaments and Molecular Motor Proteins in Giant Liposomes. *Langmuir*, 24(20):11323–11326, October 2008.

[28] YC Tan, K Hettiarachchi, M Siu, YR Pan, and AP Lee. Controlled microfluidic encapsulation of cells, proteins, and microbeads in lipid vesicles. *J. Am. Chem. Soc*, 128(17):5656–5658, 2006.

[29] Shia-Yen Teh, Ruba Khnouf, Hugh Fan, and Abraham P Lee. Microfluidic Formation of Monodispersed and Uniform Lipid Vesicles for Artificial Cell Studies. *In submission.*

[30] Shia-Yen Teh, Robert Lin, Lung-Hsin Hung, and Abraham P Lee. Droplet microfluidics. *Lab on a Chip*, 8(2):198, January 2008.

[31] A S Utada, E Lorenceau, D R Link, P D Kaplan, H A Stone, and D A Weitz. Monodisperse double emulsions generated from a microcapillary device. *Science*, 308(5721):537–541, April 2005.

[32] Peter Walde. Building artificial cells and protocell models: Experimental approaches with lipid vesicles. *BioEssays*, 32(4):296–303, March 2010.

[33] Peter Walde, Katia Cosentino, Helen Engel, and Pasquale Stano. Giant Vesicles: Preparations and Applications. *ChemBioChem*, 11(7):848–865, March 2010.

[34] T Yoshitani. Water permeabilityoflipidmembranes ofGUVs and itsdependence on actin cytoskeletons inside the GUVs. *... and Human Science*, 2008.

[35] Y Zhang, WC Ruder, and PR LeDuc. Artificial cells: building bioinspired systems using small-scale biology. *Trends in biotechnology*, 26(1):14–20, 2008.

[36] J ZHAO, J WU, F HEBERLE, T MILLS, P KLAWITTER, G HUANG, G COSTANZA, and G FEIGENSON. Phase studies of model biomembranes: Complex behavior of DSPC/DOPC/Cholesterol. *Biochimica et Biophysica Acta (BBA)-Biomembranes*, 1768(11):2764–2776, November 2007.